Najeeb M. A. Rasul · Ian C. F. Stewart *Editors*

Geological Setting, Palaeoenvironment and Archaeology of the Red Sea

هيئة المساحة الجيولوجية السعودية
SAUDI GEOLOGICAL SURVEY
www.sgs.org.sa

Springer

Geological Setting, Palaeoenvironment and Archaeology of the Red Sea

Najeeb M. A. Rasul • Ian C. F. Stewart
Editors

Geological Setting, Palaeoenvironment and Archaeology of the Red Sea

هيئة المساحة الجيولوجية السعودية
SAUDI GEOLOGICAL SURVEY
www.sgs.org.sa

Springer

Editors
Najeeb M. A. Rasul
Center for Marine Geology
Saudi Geological Survey
Jeddah, Saudi Arabia

Ian C. F. Stewart
Stewart Geophysical Consultants Pty. Ltd.
College Park, SA, Australia

ISBN 978-3-319-99407-9 ISBN 978-3-319-99408-6 (eBook)
https://doi.org/10.1007/978-3-319-99408-6

Library of Congress Control Number: 2018952604

This Springer imprint is published by the registered company Springer Nature Switzerland AG
The registered company address is: Gewerbestrasse 11, 6330 Cham, Switzerland

Preface

The Red Sea has a unique tectonic history, environment and biology. It is a young ocean basin that along its length has undergone or is undergoing the transition from a continental rift to true oceanic seafloor spreading, the nature of which is still open to vigorous debate. In addition, due to its semi-enclosed nature and location within an arid region, the environment is affected by high evaporation rates that, together with limited contact with the Indian Ocean, result in high temperatures and salinities. Lower sea levels in the past have also led to extensive evaporite deposition within its basin, while brines and metallic deposits in the axial deeps have been the subject of considerable research. All of this has had a far-reaching impact on the marine and terrestrial life of the region and on its human inhabitants. As a human environment, the Red Sea region is of unusual archaeological and historical interest. It has always been the primary gateway for contact and movement between Africa and Asia, beginning far back in the Quaternary with the earliest expansion of our human ancestors out of Africa, and in later periods becoming a primary conduit for seaborne trade between southern Asia, Arabia, Africa and the Mediterranean.

This is one of a pair of volumes that together represent a successor to an earlier volume published in this series in 2015 under our joint editorship as 'The Red Sea: The Formation, Morphology, Oceanography and Environment of a Young Ocean Basin'. The amount of new information that has become available since then is testament to the range and vigour of new research now being carried out in the region, much of it in Saudi Arabia under the sponsorship of the Saudi Geological Survey, and to the level of international interest. Indeed, so much new research has taken place that we have divided the material into two volumes, this one, which concentrates on geological, environmental and archaeological issues, and a second volume concerned with the oceanography and biology of the Red Sea.

A wide range of topics is examined in this volume, from the geological history of the region to its past and present environments and their effects on prehistoric and historic human activities. The chapters aim to present some of the current thinking and summaries of research in each field of study including useful reference lists for further study.

As with the earlier volume referred to above, which was the outcome of a workshop held in Jeddah, Saudi Arabia, in 2013, most of the chapters in this volume were originally presented at a workshop held in Jeddah, from 15 February to 17 February 2016, under the auspices of the Saudi Geological Survey (SGS), and have been extensively rewritten, independently reviewed and edited for publication.

The support of the Survey in the preparation of this volume is greatly appreciated, and we would like to thank all those who have been involved in its production. We would especially like to thank Dr. Zohair A. Nawab, former President of SGS, and Dr. Abdullah M. Alattas, former Assistant Vice President, as well Eng. Hussain M. Al Otaibi, President of SGS and Mr. Salah A. AlSefry, Assistant Vice President for Technical Affairs. Colleagues at the SGS and the Center for Marine Geology are also thanked for making the workshop a success. Mr. Louiesito Abalos played a substantial part in the preparation of material for publication. We are happy to note our appreciation for the contributions of the technical referees who

improved the contents of the chapters as well as the assistance of Femina Joshi Arul Thas, Project Manager, Banu Dhayalan, Project Coordinator, Janet Sterritt-Brunner, Production Books Project Coordinator and Dr. Nabil Khélifi, Senior Editor, of Springer Nature. The assistance and suggestions of Dr. Geoff Bailey, in particular, in preparing some of the chapters greatly helped in the final stages of the reviewing process.

Jeddah, Saudi Arabia — Najeeb M. A. Rasul
College Park, Australia — Ian C. F. Stewart

Contents

Introduction to Geology, Palaeoenvironment and Archaeology of the Red Sea

Najeeb M. A. Rasul, Ian C. F. Stewart, Geoff N. Bailey, and Zohair A. Nawab

1 Introduction

The present volume follows on from an earlier work edited by Rasul and Stewart (2015), in which an extensive introduction (Rasul et al. 2015) outlined the main features of the Red Sea, including an overview of the regional tectonics, geology and geophysics, oceanography and biology. Only one chapter in that volume referred to archaeology, and summarized knowledge then existing about the general Stone Age record with particular emphasis on the role of the Red Sea as a corridor for the earliest expansion of human populations out of Africa during the Pleistocene and the impact of Pleistocene sea-level and climate change on patterns of occupation in the Arabian Peninsula (Bailey 2015). Since that chapter was written, there has been a considerable expansion of archaeological research in Saudi Arabia involving joint Saudi-international teams under the sponsorship of the Saudi Commission for Tourism and National Heritage, along with ongoing geological investigations under the aegis of the Saudi Geological Survey.

Two major projects funded by the European Research Council have got underway in Saudi Arabia to explore in greater detail the early Stone Age history of the region: DISPERSE, focused primarily on the coastal zone of the Red Sea and the submerged landscapes made available to human occupation during periods of low sea level, and PALAEO-DESERTS, focused mainly on the desert interior and the expansion of early populations made possible by climate change. Since the likely time depth of human occupation extends back to at least 500,000 years ago and most likely much earlier still, geological and climatic changes would have had a major impact on the territory and resources available for human occupation, and of course on the preservation and visibility of archaeological data, including tectonic and volcanic activity, patterns of erosion and sedimentation, and changes in sea-level change, climate and hydrology. There is, therefore, a natural interest in common between geologists and archaeologists, and especially in obtaining improved geological control on changes in the natural environment. Both projects referred to above are multi-national, multi-disciplinary projects including specialists with a range of archaeological, geological and geochronological skills. Their results dominate the archaeological chapters in this volume, and in some cases refer as much to geological issues as to archaeological ones, and the inter-relationship between these two scientific domains.

This volume brings together some of the results of this new phase of research, with 22 chapters primarily on geological themes, and 11 chapters on primarily archaeological ones. In this introductory chapter, we briefly summarise some of the key features of the Red Sea Basin, and provide an introduction to the themes of the ensuing chapters.

2 Location, Bathymetry and Statistics

The Red Sea is a semi-enclosed, elongated warm body of water about 2000 km long with a maximum width of 355 km, a surface area of roughly 458,620 km^2, and a volume of $\sim$250,000 km^3 (Head 1987). The Red Sea is bounded by nine countries, with numerous coastal lagoons

N. M. A. Rasul (✉)
Center for Marine Geology, Saudi Geological Survey, Jeddah, Saudi Arabia
e-mail: najeeb_rasul@hotmail.com; rasul.nm@sgs.org.sa

I. C. F. Stewart
Stewart Geophysical Consultants Pty. Ltd, Adelaide, SA 5069, Australia
e-mail: stewgeop@senet.com.au

G. N. Bailey
Department of Archaeology, University of York, King's Manor, York, YO1 7EP, UK

G. N. Bailey
College of Humanities, Arts and Social Sciences, Flinders University, GPO Box 2100 Adelaide, SA 5000, Australia

Z. A. Nawab
Saudi Geological Survey, Jeddah, Saudi Arabia

N. M. A. Rasul and I. C. F. Stewart (eds.), *Geological Setting, Palaeoenvironment and Archaeology of the Red Sea*,
https://doi.org/10.1007/978-3-319-99408-6_1

and a large number of islands of various dimensions and extensive groups of shoals; it is bifurcated by the Sinai Peninsula into the Gulf of Aqaba and the Gulf of Suez at its northern end (Fig. 1). The sea is connected to the Arabian Sea and Indian Ocean via the Gulf of Aden in the south through the narrow Strait of Bab el Mandab, which has a minimum width of only 30 km, where the main channel is about 310 m deep and 25 km wide at Perim Island (Morcos 1970). Although the Hanish Sill at 13°44'N has a maximum depth of only 137 m, it is likely that the Red Sea has remained connected to the Gulf of Aden for at least the past 400,000 years (Lambeck et al. 2011). However, during the Last Glacial Maximum (LGM), the water depth over the Hanish Sill is estimated to have fallen to only 25–33 m (Biton et al. 2008; Lambeck et al. 2011), with considerable effects on the Red Sea circulation and ecology (Trommer et al. 2011).

The Red Sea has three distinct depth zones; shallow shelves less than 50 m in depth (about 25%), deep shelves depth ranging between 500 and 1000 m, and the central axis with depths between 1000 and 2900 m. The continental slope has an irregular profile, with a series of steps down to about 500 m depth. The 15% of the Red Sea that forms the narrow axial trough is over 1000 m in depth and contains the bathymetric depressions or deeps, some containing hot saline brines (e.g., Hovland et al. 2015) and metalliferous sediments, that were formed by the spreading of the sea; recent data along the axis (Augustin et al. 2014) suggest that the western Suakin Deep, with a depth of 2860 m at 19.6°N is the deepest part of the Red Sea Rift.

The Red Sea is one of the youngest oceanic zones on earth, and together with the Gulf of Aqaba-Dead Sea transform fault it forms the western boundary of the Arabian plate, which is moving in a north-easterly direction. The plate is bounded by the Bitlis Suture and the Zagros fold belt and subduction zone to the north and northeast, and the Gulf of Aden spreading centre and Owen Fracture Zone to the south and south-east (Fig. 2, modified after Stern and Johnson 2010). Along most of its length the Red Sea forms a rift through the Precambrian Arabian-Nubian shield. The Red Sea is of considerable interest, as in the north it is probably undergoing the transition from crustal stretching and thinning to true seafloor spreading, while south of about 24°N the transition has already occurred. The tectonic history of the Red Sea has recently been discussed by Bonatti et al. (2015) and Bosworth (2015). In the Red Sea, the central spreading axis is opening at an average rate of about 1.6 cm per year, with the rate of opening being greater in the south than in the north, as indicated by the width of the Red Sea between the topographic shoulders of the Precambrian basement. These are about 200 km apart in the north at latitude 27°N and 350 km apart in the south at latitude 17°N.

The southern end of the Red Sea joins the Gulf of Aden spreading centre and the northern end of the East African Rift Zone at a triple junction in the Afar region, which may be underlain by an upwelling deep mantle convection plume (e.g., Daradich et al. 2003), resulting in extensive volcanism in the region. In the early stages of rifting, prior to a permanent connection to the Gulf of Aden, thick evaporite deposits accumulated in the Red Sea, and on the shelf and marginal areas these deposits are overlain by Recent sediments. The sea only turned into an open marine environment when the Gulf of Suez in the north and Indian Ocean in the south became connected in the Pliocene.

In the north, the Red Sea bifurcates into the Gulf of Aqaba and Gulf of Suez, where it connects to the Mediterranean Sea via the Suez Canal. The seismically active Gulf of Aqaba is 160–180 km long and 19–25 km wide, narrow in the north and widening to the south with maximum depths of 1850 m toward the east, where shelves and coastal plains are absent. It is part of a left lateral transform fault system moving at about 5–7 mm per year (Ben-Avraham et al. 2008) that forms the north-west boundary of the Arabian Plate and connects the Red Sea, where seafloor spreading occurs, with the Zagros-Taurus zone of continental collision.

The Gulf of Suez is a 300 km long, 25–60 km wide, shallow flat bedded basin with depths ranging between 50 and 75 m. Depths increase toward the south but remain under the 100-m mark at the confluence of the Red Sea and do not exceed 200 m. It is basically a failed continental rift that remains floored by continental crust, with a complex extensional system of blocks that have rotated along low-angle or listric fault planes (Bosworth 1995), with three distinct depocentres for sedimentation. Since the middle Miocene the widening of the Red Sea at its northern end has largely been accommodated by the Gulf of Aqaba-Dead Sea transform, but continuing seismicity in the southern Gulf indicates that there is still some ongoing extensional stress and associated normal faulting.

3 Chapters in this Volume

3.1 Tectonics and Geology

Regional tectonic and geological aspects of the formation of the Red Sea are discussed in the next eight chapters of this volume, followed by two chapters dealing with hydrothermal fluids, brines and salt formation in the Red Sea. Three chapters deal with offshore and onshore structure as well as more the more regional configuration of the crust across Saudi Arabia. A chapter on sediment deposition in the deep Red Sea is followed by two chapters on the fossil reef system in the Gulf of Aqaba. Various aspects of the onshore Cenozoic harrats (lava fields) and dykes are then discussed

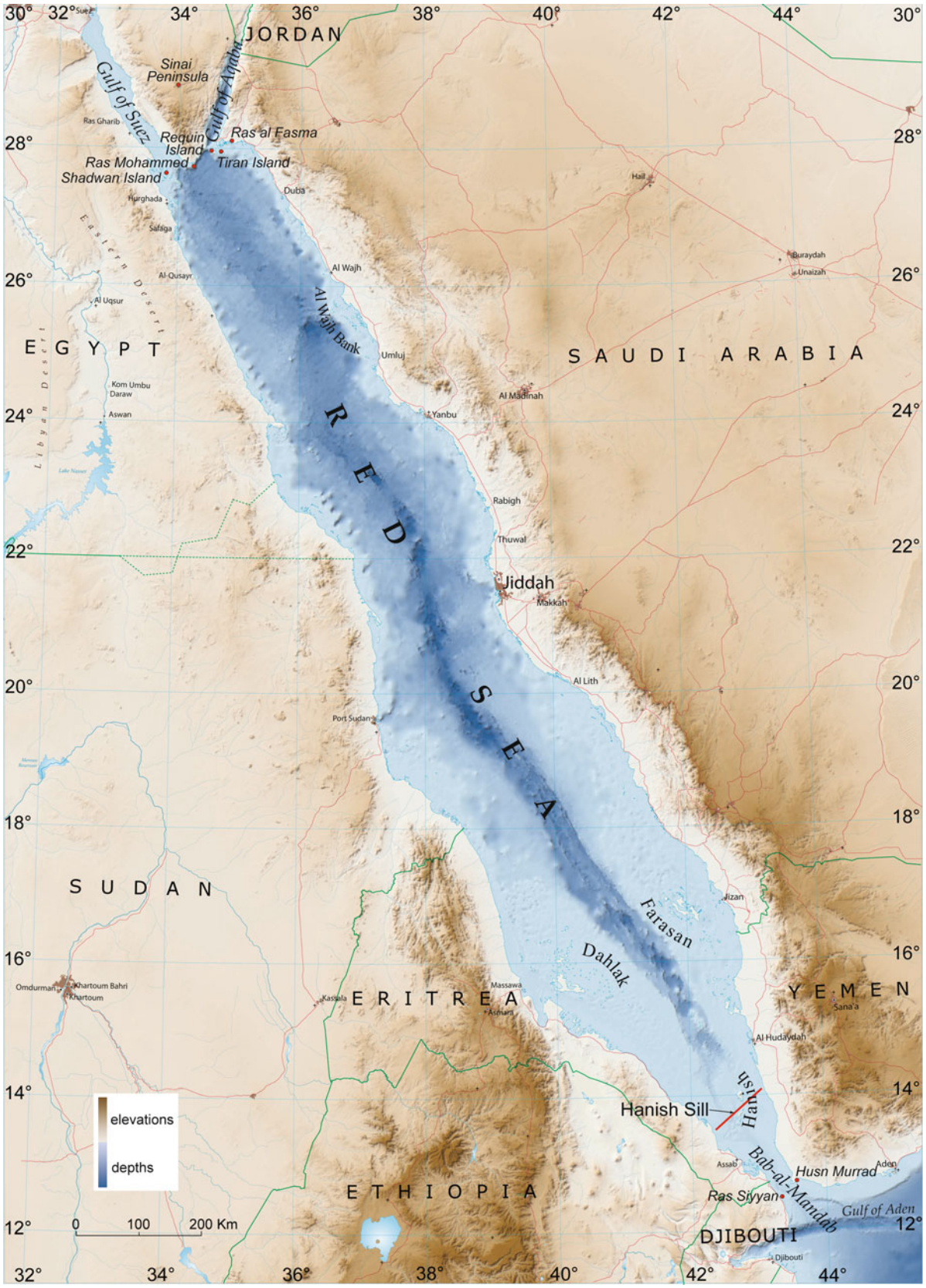

Fig. 1 Geographic map of the Red Sea area, where darker colours indicate greater depths or higher elevations (after Rasul and Stewart 2015)

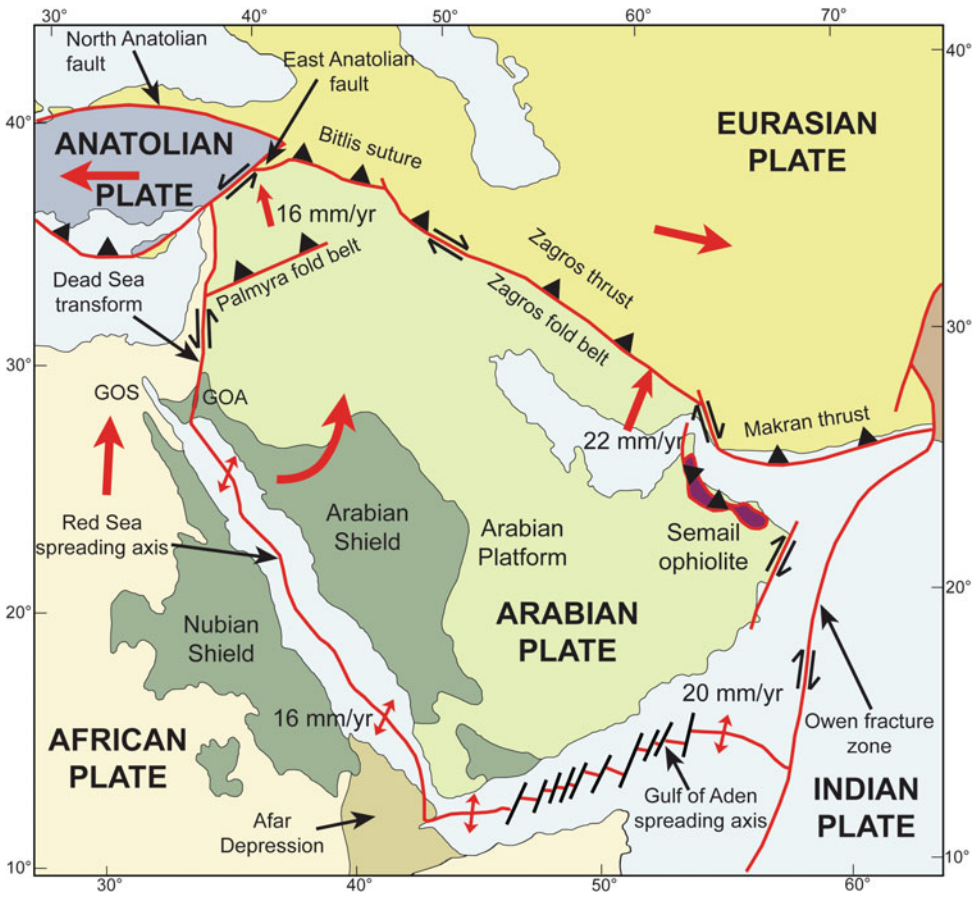

Fig. 2 Main tectonic features of the Arabian Peninsula and surrounding areas (modified from Stern and Johnson 2010)

in the next three chapters. One chapter that describes mineralisation associated with Red Sea rifting is then followed by the last two chapters in the geology section, on recent sedimentation in the Red Sea.

Bosworth et al. discuss the stress regime and ongoing and geologically recent tectonics of the Red Sea and surrounding areas, and how and where rifting and faulting is actually occurring. At the continental scale, the Red Sea is subjected to compression perpendicular to or at a high-angle to its margins. NNE–SSW extension in the southern Gulf of Suez is probably generated by sinistral slip on the similarly oriented Gulf of Aqaba transform margin. The kinematics of the southern Red Sea are complex; not all opening has jumped to the west side of the Danakil horst and significant tectonic activity still occurs along the southernmost Red Sea axis in the vicinity of the Zubair Archipelago. While the most significant neotectonic features of the Red Sea rift system are its southern oceanic spreading centre and the left-lateral Gulf of Aqaba–Levant transform fault in the north, many segments of the rift margins and in particular the Gulf of Suez remain tectonically active.

The process of rifting in the Red Sea, together with its associated volcanism at the spreading centre are described by Augustin and his colleagues. In some parts of the Red Sea the initiation of rifting is obscured by thick submarine flows that blanket the rift valley and obscure what may be a continuous rift axis rather than discrete spreading nodes between regions of continental crust. The geophysical data that was previously used to support the presence of continental crust between the axial basins with outcropping oceanic crust can be equally well explained by processes related to the sedimentary blanketing and hydrothermal alteration.

Stern and Johnson examine the onshore geology adjacent to the Red Sea and how it affects the debate about the tectonic transition from extended continental crust to true seafloor spreading. Correlations across the Red Sea between features such as sutures between tectonostratigraphic terranes, regions of transpressional shortening, and brittle-ductile faults related to Ediacaran orogenic collapse and tectonic escape that vary in orientation with respect to the coastlines require a tight pre-rift fit of the Arabian and Nubian Shields that implies that most of the Red Sea is underlain by oceanic crust. There is clear evidence for oceanic crust along the axis of the southern Red Sea, and the data is suggestive of this for the northern Red Sea.

The voluminous Eocene to Oligocene flood basalts in northern Ethiopia and western Yemen that predate Red Sea

extensional faulting and rifting are described by Stockli and Bosworth. Basaltic dike emplacement, syn-rift subsidence and sedimentation, and rapid rift-related fault block exhumation at ~23 Ma along the entire Red Sea-Gulf of Suez rift system then marked the onset of the various stages of Red Sea lithospheric extension and rifting. Middle Miocene onset of left-lateral displacement along the Gulf of Aqaba transform resulted in the tectonic isolation of the Gulf of Suez and a switch from rift-normal to highly oblique extension with the Red Sea that led to the formation of fracture zones, pull-apart basins, and crustal necking, and ultimately local crustal separation and mantle exhumation, prior to Plio-Pleistocene incipient oceanic breakup in the northern Red Sea.

The nature of upper mantle upwelling during initiation of seafloor spreading in the southern Red Sea is studied by Gallacher and his colleagues. They imaged the mantle beneath the southern Red Sea, Afar and the Main Ethiopian rift using Rayleigh-wave tomography to generate a high-resolution 3-dimensional shear-wave velocity model of the upper 250 kilometres that shows the mantle response during the progression from continental rifting to seafloor spreading. The segmented low-velocity anomalies are consistent in scale from the oceanic southern Red Sea rift to the continental Main Ethiopian rift, suggesting that mantle segmentation beneath oceanic rifts initiates early during continental rifting.

Seismic and other geophysical and geological data from the NW Red Sea and the Brothers Islets are used by Ligi et al. to provide constraints on the composition, depth of emplacement and age of early syn-rift magma intrusions into the deep crust. They suggest a stretched and thinned continental crust with few isolated sites of basaltic injections, consistent with a model whereby asthenospheric melt intrusions contribute to weaken the lower crust enabling some decoupling between the upper and lower crust, protracting upper crust extension and delaying crustal breakup. Continental rupture in the northern Red Sea is preceded by intrusion of basaltic melts that cooled forming gabbros at progressively shallower crustal depths as rifting progressed toward continental separation.

Taking a somewhat different approach, Mohriak compares rifting and salt deposition in the Red Sea with those observed in the sedimentary basins on the margins of the South Atlantic. Seismic profiles integrated with gravity and magnetic potential field data suggest alternative models for the birth of oceanic basins that evolve from an earlier phase of intracontinental rifting, salt deposition and continental breakup by mantle exhumation or by development of oceanic spreading centres preceded by igneous intrusions and extrusions in the transition from continental to oceanic crust. Alternative interpretations for syn-rift successions and salt distribution in regional seismic profiles from the Red Sea, together with well data, are compared with similar tectono-stratigraphic settings in the South Atlantic. The data suggest that the Red Sea constitutes a better analogue for the development of the South Atlantic divergent continental margins than the Iberian margin.

Plate motions around the Red Sea since the Early Oligocene are summarised by Schettino and his colleagues. The Red Sea is a very young oceanic basin that formed ~4.6 Ma, although the rifting phase started at ~30 Ma. Two kinematic stages are characterized by distinct directions of extension and different duration; in the first stage, northward motion of the Arabian plate with respect to Africa was accompanied by N–S oriented strike-slip faults and normal faults having E–W strike, with extension that was mainly accommodated by the formation of pull-apart basins. From ~27 Ma (late Oligocene), the extension axes acquired the modern NE–SW pattern, which was conserved until the early Pliocene in the southern Red Sea and is still active in the north.

Hydrothermal fluids in the rift are discussed by van der Zwan et al., with a study of Cl in the assimilation of hydrothermally altered crust at an ultra-slow spreading ridge, due to its saline seawater, the presence of hot brine pools, and the thick evaporite sequences that flank the young rift. Basaltic Cl-excess is spatially closely correlated with evidence of hydrothermal activity, suggesting that deeper assimilation of hydrothermal Cl is the dominant Cl-enrichment process. The basaltic Cl-excess can be used as a tracer together with new bathymetric maps as well as indications of hydrothermal venting (hot brine pools, metalliferous sediments) to predict where hydrothermal venting or now inactive hydrothermal vent fields can be expected.

Salt formation processes during rifting are discussed by Hovland et al. Recent observations of salt flows on the Red Sea floor and huge accumulations of salts in the sub-surface (‘Salt Walls’ and ‘Salt Ridges’), associated with topographical lows (Deeps), suggest that the Red Sea currently produces new volumes of brines and solid salts underground by boiling and supercritical phase separation in forced convection cells (hydrothermal circulation), located above shallow-seated magmatic intrusions along the spreading axis. When reaching the seafloor, the newly formed brines are cooled further, eventually becoming oversaturated in salts, which results in precipitation onto the seafloor, eventually giving rise to salt glaciers, salt walls, salt pinnacles, and ‘diapirs’ (injectites).

On a more localised topic, the possible origin of the submarine channel north of the Hanish Sill is discussed by Mitchell and Sofianos. Although the currents may help to maintain the upper channel morphology, it is unclear how they would have created the channel, nor can modern currents explain the deeper parts of the channel. The channel is straight and runs parallel with the spreading rift to the north,

suggesting that faults may underlie the channel, though a tectonic origin (graben) is not supported by Bouguer gravity anomalies, which reveal no underlying structure. The channel may have originated from massive inflow of Indian Ocean water into the Red Sea following earlier isolation and drawdown of its level.

Onshore, Cenozoic faults, mainly younger than 23 Ma, in NW Saudi Arabia are examined by Roobol and Stewart, and a number of previously unknown structures are identified, including a zone of shattered and intensely faulted rocks 25 km wide that extends inland into Saudi Arabia from the coast of the Gulf of Aqaba. A major Cenozoic fold extends 50 km inland from the coast, where the Precambrian lithologic units, dikes and faults are rotated 90° anticlockwise with the appearance of a drag fold due to the approximately 115 km sinistral offset of the Gulf of Aqaba that probably resulted from the initial displacement of the Arabian Plate from Sinai. Aeromagnetic anomalies show that the traces of major Tertiary gabbro dikes that parallel the Red Sea coast of Saudi Arabia are also curved within the fold, but their curvature of about 45° anticlockwise is less than that of the Precambrian rocks and dikes, which suggests dike emplacement occurred after folding commenced.

In a seismological study, Mai and his colleagues use receiver-functions and surface-wave dispersion curves to determine the crustal and upper-mantle structure of Saudi Arabia, showing first-order differences in crustal thickness between the Arabian Shield in the west and the Arabian Platform in the east. Moho depths generally increase eastward, while crustal thickness varies strongly in the west over the volcanic regions and near the Red Sea. The data refute the hypothesis of a small localized mantle plume as the origin for the volcanic activity in western Saudi Arabia and suggest that the volcanism in western Arabia may be due to the lithospheric mantle being heated from below by lateral flow from the Afar and (possibly) Jordan plumes.

Mitchell et al. examine the deep-water Plio-Pleistocene sediments in the Red Sea, where the sediment distribution does not reflect the pattern of sediment input from the positions of wind gaps through the Red Sea hills and fluvial drainage basin outlets. Near the coast of Egypt, 3D seismic data shows that sediment deposition is unrelated to drainage basins of the adjacent hills, but is strongly affected by halokinetics, with sediment filling evaporite depressions that are elongated sub-parallel with the coast. Profiler data of Pleistocene sedimentation around the Thetis Deep suggests that hemipelagic sedimentation has been almost uniform, and also reveals localized slope failure and sediment flow deposits, as well as tectonic disruptions. The slope failures occurred in the Late Pleistocene after Marine Isotope Stage (MIS) 12 and probably before MIS 6, probably because of seismic ground accelerations. From potential acceleration and earthquake magnitudes, the results suggest that the very low incidence of historical earthquakes in the central Red Sea is not entirely representative of the Late Pleistocene.

The Pleistocene raised marine terraces that occur on both sides of the Gulf of Aqaba are described by Taviani et al. The best developed marine terrace system is reefal, from the last interglacial (Marine Isotope Stage 5e = MIS 5e, $\sim$125 ka BP), although older Pleistocene terraces also occur. All such deposits are very fossiliferous and most carbonates are relatively unaltered, providing suitable material for geochronological purposes. The MIS 5e deposits reflect the structurally-controlled bedrock geology and the Gulf's topography, and the terraces sitting on the crystalline Arabian basement have been tectonically uplifted by up to 26 m above the present mean sea level. The bulk of the marine deposits represent upper fore-reef to beach settings, with back-reef to lagoonal facies only preserved where sufficient accommodation space (wadi valleys) was available during the MIS5e to allow inland marine expansion. Still on the subject of fossil reefs, Angelleti et al. describe the mollusc fauna associated with the Late Pleistocene coral reefs on the Saudi Arabian side of the Gulf of Aqaba, where the MIS 5e deposits document former back reef to fore-reef environments, as well as beach or mangal settings.

Sanfilippo et al. report on a geochemical study of rocks from Harrats Lunayyir and Khaybar, two large lava fields located in the western Arabian Peninsula. The trace element signatures are consistent with alkaline magmas produced by an enriched mantle source, akin to that producing continental flood magmatism in other locations of the Arabian-Nubian plate, with magmatic evolution that occurred in magma chambers located close to the crust-mantle boundary. The results suggest that Cenozoic alkaline volcanism in western Arabia formed mainly by decompression melting of ancient fusible components in the sub-Arabian lithospheric mantle. These were remobilized by lithospheric thinning due to Red Sea rifting and are consistent with progressive thinning of the lithosphere toward the Red Sea and lengthening of the melting column over time. The palaeomagnetism and geochronology of these two harrats are presented in the next chapter by Vigliotti et al. The results imply that the whole rotation of the Arabian Plate took place during the last phase (4–5 Ma) of the opening of the Red Sea, corresponding with true sea floor spreading.

Zanoni et al. study the microstructure and geochemistry of acidic, intermediate, and basic dykes sampled along the Arabian margin. Geochemical results indicate that basanite/basaltic dykes are compatible with a divergent environment such as the Red Sea rifting, whereas andesite dykes are compatible with a convergent setting. The rhyolitic dykes are interpreted as related to the Red Sea rifting as they show geochemical signatures compatible with divergent tectonics and are from a region where rhyolitic dykes were dated around 20 Ma.

Manganese or ferro-manganese mineralization that occurs along the western Red Sea coastal zone and Sinai, Egypt is closely associated with the Red Sea rifting, as described by El Agami. Hydrothermal manganese deposits occur as veins and fracture-filling cutting across the structure of the host rocks, indicating an epigenetic origin, and the mineral forming associations are typical for hydrothermal Mn deposits. The Miocene Mn deposits of the Abu Shaar area are formed by diagenetic replacement of the calcitic materials by Mn-bearing solutions during a marine transgression-regression, and the characteristic mineral-chemical enrichment and geochemical association indicate a marine-diagenetic origin.

One of the offshore reefs known as Shiab Al-Kabeer extends over an area of approximately 6.5 km^2 to the west of Jeddah. Rasul and Qutub have studied the nature and distribution of surface sediments on the shoal and describe sedimentation processes and the likely sources of these sediments, drawing attention to the significant roles played by sea birds, fish, and many invertebrates such as corals in terms of creating sediments. Parrotfish, pufferfish, surgeonfish and shrimp gobies play significant roles in grinding down the dead corals into coral sands, and burrowing organisms such as worms and holothurians also play important roles in recycling sediments. Algae and sponges also bore into the hard calcareous reef structure, leaving burrows and crevices. This study provides a potential model for future sedimentology both here and on other offshore reefs that are attracting the interest of tourism developers. Understanding what has created this species-rich environment will help to ensure that planners do not destroy those very aspects that initially attracted them to these isolated reefs and islands.

Finally, in the geology section, Abuabdullah and Şen study sediment yield rates from drainage basins (wadis) in Saudi Arabia adjacent to the Red Sea. Although wind deposition plays a significant role, the bulk of the sediment yield is due to surface water runoff after each storm rainfall. Drainage basin morphological variables including the basin area, basin slope, main channel slope and the drainage density are used to calculate the sedimentation rates for 3 wadi systems on the Saudi Arabian coast.

3.2 Palaeoenvironment and Archaeology Chapters

The main group of archaeological chapters presents different results from the DISPERSE project, and focuses on the earliest archaeological evidence for human presence along the Red Sea escarpment and the role of coasts and coastal environments in facilitating the expansion of early Stone Age populations out of Africa.

Sinclair et al. present the results of recent archaeological surveys in the south-west provinces of Jizan and Asir, discuss the dating of the important stratified sites of Dhahaban Quarry and Wadi Dabsa, and examine the stone tool assemblages at these locations in relation to their palaeoenvironmental setting. The large number of stone artefacts, and technological and typological differences indicating a wide range of ages, suggest that these were especially attractive locations in the wider landscape, repeatedly visited over long periods of the Pleistocene, most probably because of their association with strategic positions for monitoring the movements of large mammals and facilitating their capture, with nearby sources of basaltic rock for making stone tools, stream channels and water sources. At Wadi Dabsa, lava flows circumscribe an extensive tufa-filled basin, suggesting perennial supplies of slow-moving water that would have made an attractive magnet for animal and human populations. At Dhahaban Quarry, proximity to a palaeo-coastline suggests the additional possibility of exploiting resources along the sea shore.

Inglis et al. report the results of a combined geological and archaeological survey of elevated coral reefs in the same region and on the Farasan Islands, with details of location, elevation, collection of dating samples and archaeological associations. These reefs are of interest both as markers of former high sea level positions, as evidence for late Quaternary tectonic movements, as chronological markers for associated stone tools, and as former coastal environments of potential significance to the Stone Age human populations. On the mainland coastline of Asir, the reef and beachrock elevations indicate a high sea-level stand of about 7 m asl, similar to the evidence of coral reefs reported to the north, and are compatible with an MIS 5e age ($\sim$125 ka), although independent geochronological confirmation is still awaited. These elevations are significantly higher than the MIS 5e sea level predicted by modelling of isostatic adjustment in the Red Sea, indicating either evidence of tectonic uplift over the past 125 kyr, or the need for adjustment of the isostatic model. On the Farasan Islands, reef elevations are more variable, reflecting the effects of salt tectonics.

Bailey et al. look more broadly at the issues of early coastal colonization, examine the arguments for and against early sea crossings at the southern end of the Red Sea when sea level was lower and discuss the significance of now submerged coastal landscapes and submerged palaeoshorelines. They present new information on the mid-Holocene shell mounds of the Farasan Islands and their relationship to geodynamic and ecological changes in shorelines as a case study in analysing the factors that determine the preservation and visibility of archaeological deposits in coastal settings. They refer to some of the results of underwater investigation reported in other chapters (Momber et al., Sakellariou et al.) and highlight the importance of taking into account issues of

site formation, preservation and visibility when attempting to interpret the distribution of archaeological sites in terms of palaeo-demography and environmental preferences.

Because sea levels were substantially lower than at present during the late Pleistocene and early Holocene, extensive areas were available for human settlement before being inundated by sea-level rise. Studies in other parts of the world show that coastal archaeological sites such as shell middens can survive inundation and can be discovered by underwater investigation. Momber et al. pursue this line of research and take the archaeological story under water around the Farasan Islands. They describe the range of diving techniques, remote-sensing equipment and other methods used in underwater explorations of the Red Sea and the results of underwater surveys for submerged palaeoshorelines and shell mounds in the Farasan Islands.

All these chapters refer to the results of the R/V Aegaeo survey of the deeper shelf around the Farasan Islands, and the next chapter by Sakellariou et al. gives a more detailed account. This survey was inspired by archaeological questions as part of the DISPERSE project, and though its results provide new data on the geological structure and dynamics of the outer shelf region, they also present new information about the nature of the now-submerged landscapes and topography available to Stone Age hunters and gatherers during the low sea-level episodes of the Last Glacial period. The results give new information on the MIS 3 and MIS 2 submerged coral terraces of the Farasan shelf and evidence of faulting linked to extensional tectonics and mobility of Miocene evaporites. Fault-bounded basins on the shelf associated with evidence of lacustrine sediments, and the presence of narrow valleys that must have been created by sub-aerial erosion by water action, indicate a complex topography with minor barriers, narrow valleys and sources of water that would have created attractive conditions for large animals and their human hunters.

Kübler et al. take up the theme of complex topography and the role of active tectonics and volcanism in creating attractive landscapes for early human evolution and dispersal. They range widely across the Afro-Arabian rift system, drawing on examples of early Stone Age sites and environments in the Kenyan Rift, the Dead Sea Rift, and the Arabian escarpment, the latter including reference to the Wadi Dabsa site described in earlier chapters. They show how modelling of fault motions can aid the reconstruction of an earlier topography, and further demonstrate the importance of tectonic and volcanic features and the edaphic properties of different rock and sediment types as constraints on the seasonal migrations of large mammals that facilitated ambush hunting by early Stone Age hunters.

Finally, in this archaeological grouping, Petraglia et al. summarise the results of the PALAEODESERTS project. They emphasise the important role of episodic climate change during the Pleistocene and 'greening' of the desert interior, which periodically opened up large areas of the Arabian Peninsula to settlement and dispersal following water courses and lakes, and they contrast this model of dispersal through the interior with the models of coastal dispersal examined in the previous chapters. They summarise palaeoclimatic research that demonstrates the time depth of these wetter climatic episodes, which can be identified well back into the Pleistocene, and present evidence for stratified Stone Age sites associated with palaeo-lakes, the earliest in the Nefud region dating back to 211 ka, and a palaeontological site with a large mammal fauna of mixed Eurasian and African affinity dated somewhat earlier and possibly as early as 500 ka.

Dating deposits is a perennial challenge for geologists and archaeologists, and Sanderson and Kinnaird explain the principles and techniques of Optically Stimulated Luminescence (OSL) dating and summarise the growing number of applications of this technique to the dating of palaeoclimatic sequences in the Arabian Peninsula. They also present the result of OSL dating of sediments on land and from underwater cores collected as part of the DISPERSE project. Their results have provided additional constraints on the chronology of some of the Stone Age sediments and sites examined on the Jizan/Asir mainland, and confirmed a Last Glacial Maximum age for lacustrine deposits found in the lower sections of the R/V Aegaeo cores recovered from the Farasan shelf.

The two chapters by Geraga et al. and Hausmann et al. turn the discussion to issues of palaeoclimatic reconstruction. Geraga et al. analyse changes in foraminiferal composition through a radiocarbon-dated sequence of marine sediments in one of the cores recovered from the outer Farasan shelf by the R/V Aegaeo. Their results show interesting changes through the late Pleistocene–Holocene sequence of the core, which demonstrate changes in climate, ecological productivity and oceanographic conditions at that location in the Red Sea, mainly associated with changes in sea-level and the resulting changes in the flow of currents between the Red Sea and the Indian Ocean.

Hausman et al. discuss the application of stable isotope $\delta^{18}O$ and element-ratio variations to the microscopic growth structures of marine mollusc shells recovered from the archaeological shell-mound deposits of the Farasan Islands. These techniques have, in the past, been limited in their application to archaeological shell deposits because of the costs involved and the small sample sizes of measurements that are possible. Hausmann et al., however, show how new techniques are making possible cheaper and more rapid analysis of large samples. These records can provide a very high-resolution climatic record. They can also inform on the season of collection of the molluscs, providing valuable information about the palaeodiet of the human population

and patterns of settlement. In discussing the archaeological implications of this technique, the authors return the discussion to its original starting point about the role of coastlines and coastal environments in the chapters that opened this archaeological section.

The last chapter in this archaeological section, by Kotarba-Morley, takes the discussion in a new direction and to a more recent period of Red Sea history and examines the Greco-Roman ports of trade in the Red Sea, which played such a vital role in the trade routes between Asia, southern Arabia, East Africa and the Mediterranean. She focuses on the Egyptian coastal town of *Berenike Troglodytica* and analyses a comprehensive range of variables at the site and its surroundings, including environmental parameters, agricultural productivity, water supplies, sea conditions and socio-political factors, in order to understand the rationale for the choice of location as a port town. Amongst other features of this research is the important point that dynamic changes in coastal environments and geomorphology are not only of relevance to the longer time spans of the Stone Age but play an equally important role and demand an equivalent degree of specialist investigation and analysis in the historical period.

References

Augustin N, Devey CW, van der Zwan FM, Feldens P, Tominaga M, Bantan RA, Kwasnitschka T (2014) The rifting to spreading transition in the Red Sea. Earth Planet Sci Lett 395:217–230. https://doi.org/10.1016/j.epsl.2014.03.047

Bailey GN (2015) The evolution of the red sea as a human habitat during the quaternary period. In: Rasul NMA, Stewart ICF (eds) The Red Sea: the formation, morphology, oceanography and environment of a young ocean basin. Springer Earth System Sciences, Berlin Heidelberg, pp 595–610. https://doi.org/10.1007/978-3-662-45201-1_34

Ben-Avraham Z, Garfunkel Z, Lazar M (2008) Geology and evolution of the southern Dead Sea Fault with emphasis on subsurface structure. Ann Rev Earth Planet Sci 36:357–387

Biton E, Gildor H, Peltier WR (2008) Red Sea during the last glacial maximum: implications for sea level reconstruction. Paleooceanography 23, PA1214. https://doi.org/10.1029/2007pa001431

Bonatti E, Cipriani A, Lupi L (2015) The Red Sea: birth of an ocean. In: Rasul NMA, Stewart ICF (eds) The Red Sea: the formation, morphology, oceanography and environment of a young ocean basin. Springer Earth System Sciences, Berlin Heidelberg, pp 29–44. https://doi.org/10.1007/978-3-662-45201-1_2

Bosworth W (1995) A high-strain rift model for the southern Gulf of Suez (Egypt). Geol Soc London, Spec Publ 80:75–102

Bosworth W (2015) Geological evolution of the Red Sea: Historical background, review, and synthesis. In: Rasul NMA, Stewart ICF (eds) The Red Sea: the formation, morphology, oceanography and environment of a young ocean basin. Springer Earth System Sciences, Berlin Heidelberg, pp 45–78. https://doi.org/10.1007/978-3-662-45201-1_3

Daradich A, Mitrovica JX, Pysklywec RN, Willett SD, Forte AM (2003) Mantle flow, dynamic topography, and rift-flank uplift of Arabia. Geology 31:901–904

Head SM (1987) Red Sea fisheries. In: Edwards AJ, Head SM (eds) Red Sea: Key Environments. Pergamon Press, Oxford, pp 363–382

Hovland M, Rueslåtten H, Johnsen HK (2015) Red Sea salt formations—a result of hydrothermal processes. In: Rasul NMA, Stewart ICF (eds) The Red Sea: the formation, morphology, oceanography and environment of a young ocean basin. Springer Earth System Sciences, Berlin Heidelberg, pp 187–203. https://doi.org/10.1007/978-3-662-45201-1_11

Lambeck K, Purcell A, Flemming NC, Vita-Finzi C, Alsharekh AM, Bailey GN (2011) Sea level and shoreline reconstructions for the Red Sea: isostatic and tectonic considerations and implications for hominin migration out of Africa. Quatern Sci Rev 30:3542–3574

Morcos SA (1970) Physical and chemical oceanography of the Red Sea. Oceanogr Mar Biol Ann Rev 8:73–202

Rasul NMA, Stewart ICF (eds) (2015) The Red Sea: The formation, morphology, oceanography and environment of a young ocean basin. Springer Earth System Sciences, Berlin Heidelberg, 633 pp, ISBN 978-3-662-45200-4, ISBN 978-3-662-45201-1 (eBook). https://doi.org/10.1007/978-3-662-45201-1_1

Rasul NMA, Stewart ICF, Nawab ZA (2015) Introduction to the Red Sea: its origin, structure and environment. In: Rasul NMA, Stewart ICF (eds) The Red Sea: the formation, morphology, oceanography and environment of a young ocean basin. Springer Earth System Sciences, Berlin Heidelberg, pp 1–28. https://doi.org/10.1007/978-3-662-45201-1_1

Stern RJ, Johnson PR (2010) Continental lithosphere of the Arabian Plate: A geologic, petrologic, and geophysical synthesis. Earth-Sci Rev 101:29–67

Trommer G, Siccha M, Rohling EJ, Grant K, van der Meer MTJ, Schouten S, Baranowski U, Kucera M (2011) Sensitivity of Red Sea circulation to sea level and insolation forcing during the last interglacial. Climate of the Past 7:941–955. https://doi.org/10.5194/cp-7-941-2011

Neotectonics of the Red Sea, Gulf of Suez and Gulf of Aqaba

William Bosworth, Marco Taviani, and Najeeb M. A. Rasul

Abstract

The Red Sea, Gulf of Suez, and Gulf of Aqaba comprise the active plate boundaries that separate Africa-Nubia, Arabia and Sinai. This tripartite configuration has been in existence since the Middle Miocene, or about the past 12–14 Ma. We describe the ongoing and geologically recent tectonics of these regions. The Red Sea rift lies east of a broad region of E-W maximum horizontal stress (S_{Hmax}) that covers much of central Africa-Nubia. On its Arabian side, S_{Hmax} is oriented N-S to NE-SW. These far field stresses owe their origins to the spreading centres of the Atlantic Ocean and collision between Arabia and Eurasia along the Bitlis-Zagros suture. At the continental scale, the Red Sea is therefore subjected to compression perpendicular to or at a high-angle to its margins. The realm of shallow crustal stresses conducive to extensional faulting in a Red Sea orientation (rift-normal S_{hmin}) is presently restricted to the Red Sea marine basin itself, and perhaps narrow belts along its shoulders. In the Gulf of Suez there is enough data to show that each of its sub-basins is presently undergoing extension, but in conjunction with differently oriented, sub-regional shallow crustal stress fields. These appear to be spatially related to the original Early Miocene syn-rift basin geometries. NNE-SSW extension in the southern Gulf of Suez is probably generated by sinistral slip on the similarly oriented Gulf of Aqaba transform margin. Large $M > 6$ earthquakes are generally restricted to the central basin of the Gulf of Aqaba, the southern Gulf of Suez, and the greater Afar region. The geodynamic details responsible for the focusing of these large events are specific to each locale but all are in general associated with the junctions of major plate boundaries. Catalogues of earthquake activity and GPS datasets show that the Sinai micro-plate is still moving away from Africa with a component of left-lateral slip. This results in components of extension perpendicular to both the Gulf of Suez and the Gulf of Aqaba. The kinematics of the southern Red Sea are similarly complex. Not all opening has jumped to the west side of the Danakil horst and significant tectonic activity still occurs along the southernmost Red Sea axis in the vicinity of the Zubair Archipelago. This is the only volcanically active segment of the Red Sea basin that is above sea level. Dike intrusions are ~N-S and not aligned parallel to the rift axis and may indicate that the underlying magmatism is swinging to the west to link with the Afar triple junction. All of the margins of the Red Sea, Gulf of Suez and Gulf of Aqaba underwent tectonically-driven rift shoulder uplift and denudation in the past, particularly during the main phases of continental rifting. However, during the past 125 kyr uplift has been focused along the footwalls of a few, active extensional faults. These include the Hammam Faraun-Tanka fault in the central Gulf of Suez, the Gebel el Zeit-Shadwan Island fault in the southern Gulf of Suez, the Sinai and Arabia coastal boundaries of the Gulf of Aqaba, and faults at Tiran Island at the junction of the Gulf of Aqaba and northern Red Sea. Smaller-scale extensional faulting is also occurring along the Saudi Arabian margin of the northern Red Sea, in the Dahlak and Farasan Archipelagos, and on the volcanically active islands of the Zubair Archipelago in the southernmost

W. Bosworth (✉)
Apache Egypt Companies, 11 Street 281 New Maadi, Cairo, Egypt
e-mail: bill.bosworth@apacheegypt.com; bill.bosworth@apachecorp.com

M. Taviani
Istituto di Scienze Marine (ISMAR-CNR), Via Gobetti 101, 40100 Bologna, Italy

M. Taviani
Biology Department, Woods Hole Oceanographic Institution, 266 Woods Hole Road, Woods Hole, MA 02543, USA

M. Taviani
Stazione Zoologica Anton Dohrn, Villa Comunale, 80121 Naples, Italy

N. M. A. Rasul
Center for Marine Geology, Saudi Geological Survey, Jeddah, Saudi Arabia

N. M. A. Rasul and I. C. F. Stewart (eds.), *Geological Setting, Palaeoenvironment and Archaeology of the Red Sea*,
https://doi.org/10.1007/978-3-319-99408-6_2

Red Sea. On the Farasan and Dahlak islands this is largely related to the movement of underlying salt bodies, similar to effects documented along the coastal plain of Yemen. Though not active at the present time, a broad belt of small-offset, very linear extensional faults dissected the western margin of the central Gulf of Suez during the Plio-Pleistocene. Similar age and style deformation has not been identified in the Suez sub-basins to the north or south. The most significant large-scale neotectonic features of the Red Sea rift system are its southern oceanic spreading centre and the northern linkage to the left-lateral Gulf of Aqaba—Levant transform fault. However, many segments of the rift margins and in particular the Gulf of Suez remain tectonically active. These areas provide stress field and horizontal and vertical displacement data that are relatively inexpensive to acquire and complementary to analyses of the offshore main plate boundaries themselves.

1 Introduction

This paper summarizes neotectonic features of the Red Sea, Gulf of Suez and Gulf of Aqaba (Fig. 1). These three basins, together with Afar, encompass the plate boundaries that now separate Africa-Nubia from Arabia. This configuration has been in place for about the past 12–14 Myr, since the Middle Miocene, when the Gulf of Aqaba—Dead Sea transform plate boundary came into existence. Prior to this, based on regional stratigraphic correlations, the Red Sea and Gulf of Suez were interconnected basins, dominated by open- to marginal-marine sedimentation (Tewfik and Ayyad 1984; Miller and Barakat 1988; Montenat et al. 1988; Hughes and Beydoun 1992; Hughes et al. 1992; Bosworth et al. 1998). With initiation of the transform boundary, extension rates across the Gulf of Suez dropped dramatically but not completely (Joffe and Garfunkel 1987; Steckler et al. 1988; Bosworth et al. 1998). From the Serravallian (late Middle Miocene) onward the north-easternmost boundary of Africa-Nubia involved the additional complexity of the movement of the Sinai micro-plate.

The most tectonically active part of the Red Sea rift system lies in the offshore, along the well-defined spreading centre in the south and its equivalent, though more enigmatic rift axis in the north. A wealth of new data are available for these realms (e.g., Mitchell et al. 2010; Ligi et al. 2012, 2015; Feldens and Mitchell 2015; Ehrhardt and Hübscher 2015). However, localized deformation continues along the rift flanks and as these regions are more accessible this offers a useful complementary picture to the submerged activity. A similar situation exists in the Gulf of Aqaba, where strike-slip faulting is occurring along the offshore basin axis, whereas extensional faulting is dominant in the uplifted margins (Bosworth et al. 2017).

We first review the present understanding of the relative movements between Africa-Nubia, Arabia and Sinai. This is based on geodetic, seismic, and geologic observations. Next we discuss the present-day shallow crustal stress fields that accompany these movements and are responsible for much of the active deformation now seen in outcrop. We then illustrate the most significant neotectonic features we have examined in each segment of these plate boundaries. In some cases, structures can be constrained to be truly active or postdating specific parts of the Pleistocene; in others dating is less constrained and Pliocene activity may be included. The presentation is generally organized from north to south, with youngest or present-day features discussed first.

2 Tectonic Setting

2.1 Plate Motions

Africa and Arabia are presently diverging across the southern Red Sea at a rate of 1.7 ± 0.1 cm/yr in a NE-SW direction (Fig. 1; ArRajehi et al. 2010; 2.4 cm/yr in Reilinger et al. 2015). In the northern Red Sea this reduces to about 0.7 ± 0.1 cm/yr. Plate reconstructions suggest that these opening rates must have been about half these values prior to 11 ± 2 Ma (McQuarrie et al. 2003). This roughly corresponds with geologic evidence for the time of initiation of the Gulf of Aqaba transform boundary (14–12 Ma; Bosworth et al. 2005, and references therein). Reilinger et al. (2015) suggested that the acceleration in the Red Sea opening resulted at least partially from the completion of the oceanic spreading centre along the length of the Gulf of Aden, decoupling the Arabia and Somalia plates. Several lines of evidence therefore point to a significant reorganization of plate kinematics at roughly 14–11 Ma in the greater Red Sea—Gulf of Aden rift system. GPS and geologically derived Arabian plate boundary slip rate determinations suggest that the opening of the Red Sea since the reorganization has, within observational errors, remained constant (Reilinger et al. 2015).

Although most of the northern Red Sea opening now links to the East Anatolia fault via the Gulf of Aqaba—Dead Sea transform, Sinai continues to separate from Africa-Nubia at about 0.15 cm/yr in a NNW direction (Fig. 1; Mahmoud et al. 2005). This equates to about 0.05 cm/yr rift-normal extension and 0.14 cm/yr left-lateral shear parallel to the Gulf of Suez (discussed further below).

Motion on the transform boundary itself is estimated from GPS datasets to be about 0.44 ± 0.03 cm/yr left-lateral movement near the junction with the Red Sea (ArRajehi et al. 2010). There is also about 0.2 cm/yr of opening across the

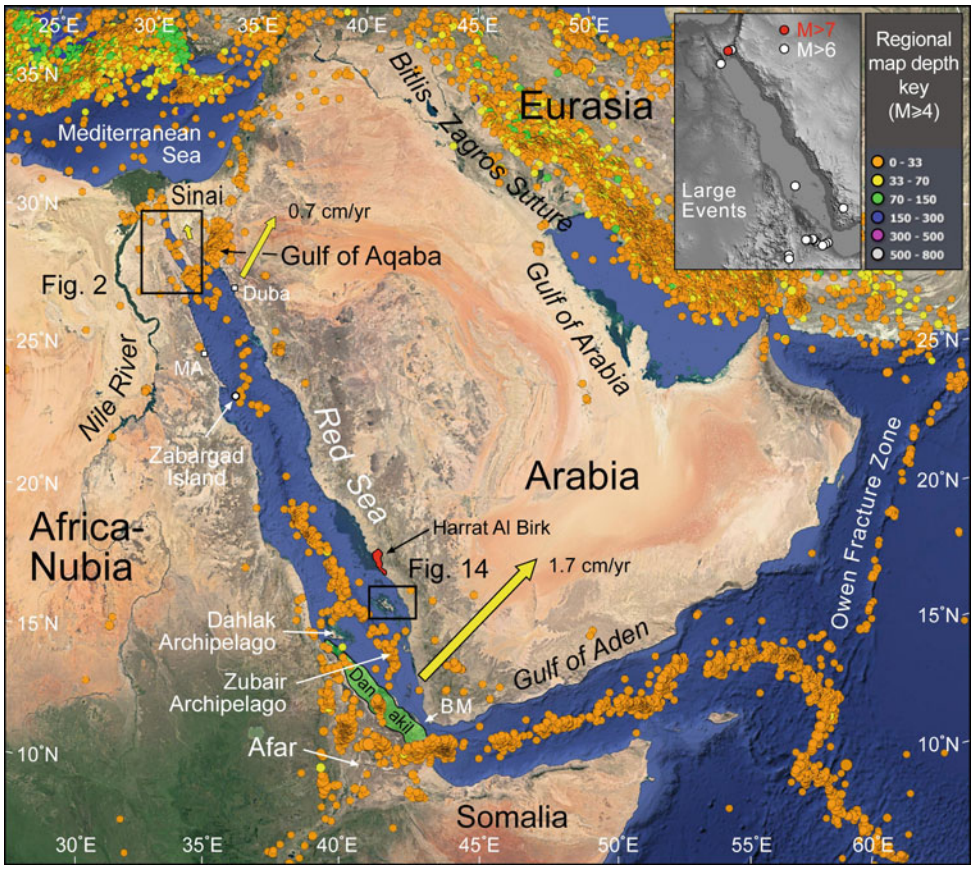

Fig. 1 Regional setting of the Red Sea, Gulf of Suez and Gulf of Aqaba. Instrumentally recorded earthquakes demarcate the plate boundaries of the region ($M \geq 4$ since 1960-01-01; ANSS 2016). Yellow arrows show the slip rates of Arabia and Sinai relative to Africa (ArRajehi et al. 2010). The small arrow on Sinai equates to 0.15 cm/yr (Mahmoud et al. 2005). Locations of Figs. 2 and 14 are shown by boxes. Volcanic rocks of Harrat Al Birk are shown in red. The continental Danakil Block is shown in green. Base is from Google Earth (Landsat/Copernicus image; data from SIO, NOAA, US Navy, GEBCO). Inset map shows positions of $M > 6$ earthquakes for the past 50 years for the Red Sea, Gulf of Suez and Gulf of Aqaba (n = 19). BM = Bab el Mandeb, MA = Marsa Alam

southern Gulf of Aqaba (Reilinger et al. 2015) which confirms its early designation as a "leaky transform" boundary (Ben-Avraham et al. 1979). As there are no syn-tectonic magmatic rocks exposed in the Gulf of Aqaba, Ben-Avraham et al. used the term leaky to indicate the creation of space perpendicular to the strike-slip boundary, without implications of volcanism. Measurements of offset pre-existing geologic features or pinning points demonstrate that total slip amounts to 107 km (Quennell 1956, 1958). Quennell thought that 62 km of this slip occurred during the Early Miocene to Pliocene, followed by a significant period of quiescence and post-Pliocene to Recent movement of an additional 45 km. The post-Pliocene rate equates to ~1.7 cm/yr. Assuming that the transform did not initiate until the time of the plate reorganization (14–11 Ma) and movement was continuous through time gives long-term averaged slip rates of 0.76–0.97 cm/yr—about twice the present GPS determination or half of Quennell's post-Pliocene rate. These disparencies suggest that the timing of Quennell's two phases of movement probably needs to be adjusted, and perhaps the time gap separating them was not as significant as he thought. It is also possible that slip along the Gulf of Aqaba has been more variable over geologic time and we are presently measuring a relatively slower period of movement. Alternatively the GPS dataset for southern Sinai is simply not robust enough to yet yield accurate instantaneous slip rates.

2.2 Seismicity

Most of the Red Sea axis and the Gulf of Aqaba presently display low to moderate levels of seismic activity (Fig. 1; Ambraseys et al. 1994; Babiker et al. 2015; ANSS 2016). A noticeable gap exists in the central part of the Red Sea at about 21–23°N latitude where no $M > 4$ earthquakes have been recorded. Overall $M > 6$ events are rare, with only 19 observed in the past 50 years (Fig. 1 inset). These larger earthquakes are focused in Afar and the central sub-basin of the Gulf of Aqaba,

although one occurred in the southern Gulf of Suez and one near the Dahlak Archipelago in the southern Red Sea. Nearly all earthquakes in this region occur in the crust at depths <33 km (ANSS 2016).

Instrumentally recorded earthquakes along the Red Sea axis generally yield normal fault solutions, although strike-slip regime solutions are clustered between the Dahlak and Farasan archipelagos (Delvaux and Barth 2010). Seismicity is locally focused at positions where the axial deep/spreading centre shifts direction (El-Isa and Al Shanti 1989). These are often interpreted as the sites of intersection of transform faults with the ridge axis.

Strike-slip fault solutions predominate for Gulf of Aqaba seismic events (Hofstetter 2003). The largest event ever instrumentally recorded in the Red Sea—Gulf of Suez—Gulf of Aqaba region occurred in the central Gulf of Aqaba on 22 November 1995 (Fig. 2). This earthquake had an interpreted M_S of 7.2 with a left-lateral strike-slip solution on a vertical NNE-SSW striking fault plane (Hofstetter 2003; ANSS 2016). However, normal fault mechanisms are also commonly observed in local network recordings (Alamri et al. 1991; Roobol et al. 1999; Hofstetter 2003). Composite focal mechanisms derived from events that occurred from 1985–1989 with M_L 2.6–3.8 indicated normal dip-slip on approximately north-south striking faults in the northern Aragonese and eastern Elat Deeps (see Fig. 8 for localities; Alamri et al. 1991). Similarly aftershock studies of the large 1995 event show that the total deformation field was complex and involved more than just sinistral strike-slip on the transform boundary fault (Roobol et al. 1999; Hofstetter 2003). Although strike-slip mechanisms predominated in the larger aftershocks, one large normal fault event occurred in the offshore north of the main epicentre. In 1993 an earthquake swarm of over 420 events occurred within and nearby the central Gulf of Aqaba deeps (Hofstetter 2003). The two largest events of the swarm (M_L = 5.8 and 5.6) were principally dip-slip. The epicentres of both of these earthquakes were located on NNE-SSW striking segments of the Arabian coastline. This is the general orientation of the Gulf of Aqaba—Dead Sea transform boundary and such structures would usually be associated with sinistral strike-slip movement. In this case the seismic events document a component of east-west extension in agreement with GPS observations discussed above.

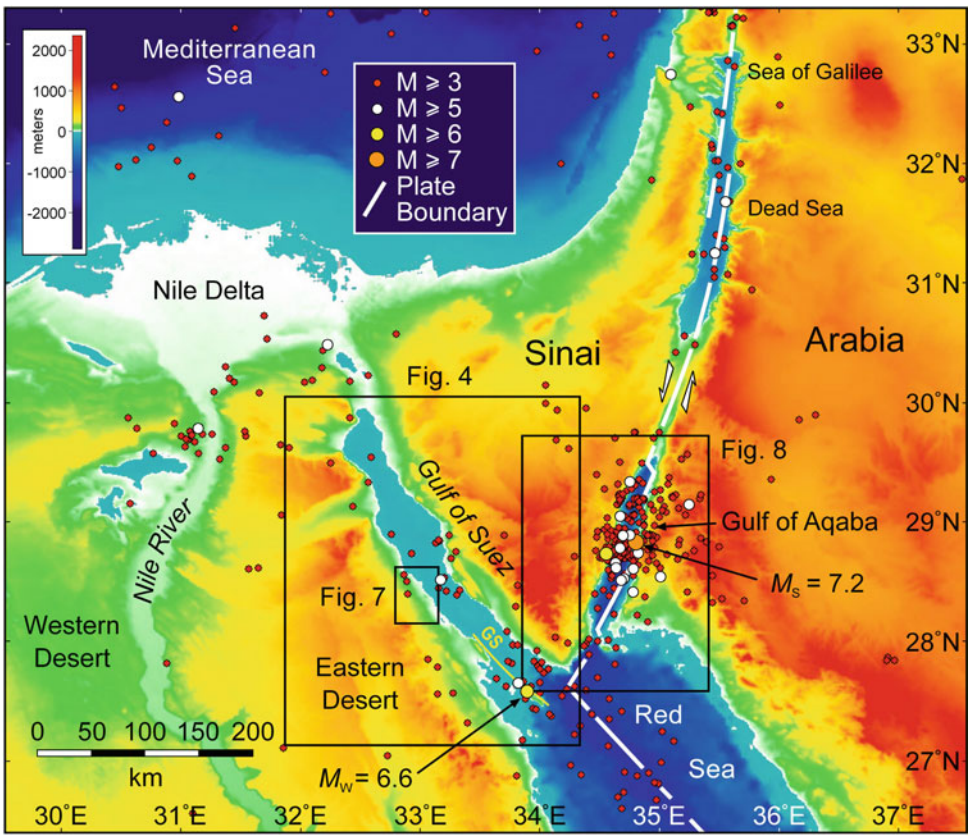

Fig. 2 Tectonic setting of the Gulf of Suez and Gulf of Aqaba and instrumentally recorded seismicity (M ≥ 3 since 1960-01-01; ANSS 2016). Base is Etopo merged bathymetry and elevations model (NOAA 2016). Line labeled GS is the Gebel el Zeit-Shadwan Island fault trend where the largest Gulf of Suez events have occurred. Positions of the M_w = 6.6 Gulf of Suez and M_s = 7.2 Gulf of Aqaba earthquakes are indicated. Location of Figs. 4, 7 and 8 are shown by boxes

Despite the fact that the Gulf of Suez is only extending at a very slow rate its seismic activity is locally much higher than most segments of the Red Sea (Figs. 1 and 2). Microseismicity is abundant in the southern Gulf of Suez, particularly for M = 1 − 3 (Daggett et al. 1986). Relatively large events were recorded in this area on 31 March 1969 (M_w = 6.6) and 28 June 1972 (M_w = 5.6) (Huang and Solomon 1987; ANSS 2016). Similarly to the earthquakes recorded in the Red Sea, these were principally normal fault events, although they have been interpreted as including a component of left-lateral shear in a NW-SE direction (Huang and Solomon 1987). This also supports the GPS interpretation that Sinai is moving both away from Africa-Nubia and toward the north.

2.3 Regional Stress Fields

The broad, regional stress field for much of the central part of the African plate displays E-W maximum horizontal stress (S_{Hmax}; Fig. 3; Zoback 1992; Bosworth 2008; Bosworth and Durocher 2017). This is based on earthquake focal mechanism determinations in West Africa (Ayele 2002; Delvaux and Barth 2010), the Sudan (Giardini and Beranzoli 1992; Gaulon et al. 1992; Delvaux and Barth 2010) and southern Egypt (Badawy 2001; Hussein et al. 2013). Industry borehole breakout data from wells in the Mesozoic Sudan rifts similarly show uniform E-W S_{Hmax} (Bosworth et al. 1992). Zoback (1992) attributed this intra-plate compression to the first-order effects of ridge push at the Central and South Atlantic and Indian Ocean spreading centres. This very broad region of relatively uniform E-W S_{Hmax} was termed the Central African Intra-plate (CAIP) stress field (Fig. 3; Bosworth 2008).

Stress field data are not available for most of the northern and central Red Sea basin. The focal mechanism inversion of Delvaux and Barth (2010) indicates NW-SE S_{Hmax}, parallel to the young spreading centre in the southernmost Red Sea (Fig. 3). Offshore Sudan, the mechanisms are normal faults, but as discussed above they become strike-slip offshore Eritrea in the vicinity of the Dahlak archipelago which is probably related to the bend of the plate boundary landward and to the west of the Danakil horst (Fig. 1).

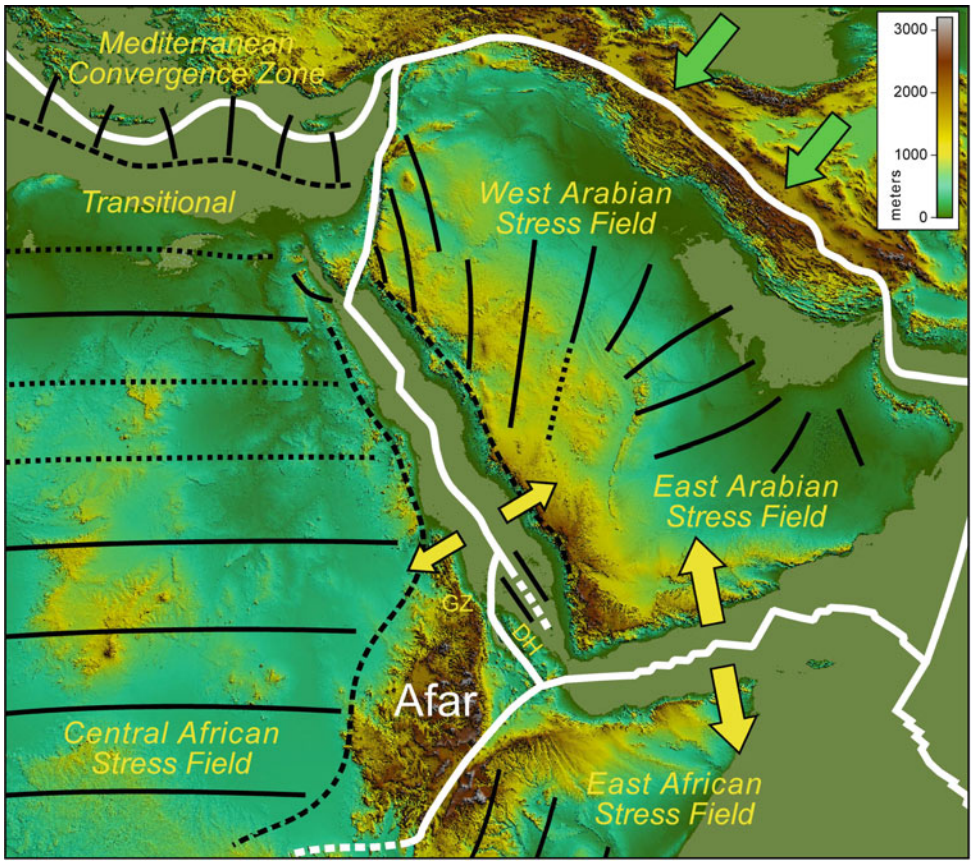

Fig. 3 Plate boundaries (heavy white lines; USGS 2016) of the greater Red Sea region and interpreted orientation of the maximum horizontal stress S_{Hmax} (Bosworth and Durocher 2017). Yellow arrows schematically represent forces from ridge-push at oceanic spreading centres and green arrows the forces associated with convergence between Arabia and Eurasia. Base is Etopo elevation model (NOAA 2016). DH = Danakil Horst; GZ = Gulf of Zula

In the Arabian Gulf region, breakout data define a fanning of S_{Hmax} from NE-SW in Saudi Arabia rotating to approximately N-S in Oman (Fig. 3; Ameen et al. 2010; Ameen 2014). The East Arabia stress field must rotate to N-S in the west as well because young volcanism in this region is being erupted from N-S aligned vents presumably overlying similarly oriented feeder dikes (Camp and Roobol 1992). The geometry of the Arabian regional stress field is strongly influenced by the nature of convergence and compression along the Bitlis-Zagros suture and its continuation into the Arabian Sea (Fig. 3). Along the Gulf of Aqaba transform boundary regional S_{Hmax} rotates further toward the NW-SE in accord with the dominant left-lateral strike-slip movement (Fig. 3; Heidbach et al. 2008). The weakness of the transform fault relative to the adjacent crust of Sinai and Arabia has been interpreted to result in S_{Hmax} swinging into parallelism with the boundary and therefore facilitating extension across the Gulf (Ben-Avraham and Zoback 1992; Bosworth et al. 2017). The stress field in the interior of the Sinai micro-plate is not yet clearly defined as earthquakes are uncommon and no outcrop or subsurface present-day stress field indicators are available.

This brief overview of the stress fields presently enveloping the Red Sea is a simplistic perspective as it does not capture the dynamic nature of this region. Sometime in the Late Pleistocene, after about 500 ka but prior to 125 ka, a significant rotation of the shallow crustal stress field occurred in the Kenya rift valley (~45° clockwise) and the northern Red Sea/Gulf of Suez (~40° counterclockwise) (Strecker et al. 1990; Bosworth et al. 1992; Bosworth and Taviani 1996; Bosworth and Strecker 1997). An adequate explanation of why these stress field rotations occurred has not been presented, nor is it clear if they were truly coeval and/or genetically related. It does suggest that care should be taken in extrapolating stress field datasets to long time intervals in the Red Sea region.

3 Sub-region Details

3.1 Gulf of Suez

Rifting in the Gulf of Suez began at ~23 Ma, at the Oligocene-Miocene transition (reviewed in Bosworth et al. 2005; Bosworth and Stockli 2016). After initiation of the Gulf of Aqaba transform boundary in the Middle Miocene, extension across the Gulf of Suez dropped dramatically to about 0.08–0.16 cm/yr based on a variety of plate circuit (Joffe and Garfunkel 1987) and geologic considerations (Steckler et al. 1988; Bosworth and Taviani 1996). Overall, extension continued to focus through time along the axis of the basin, complicated by continued movement of salt walls and domes (Moretti and Colletta 1987; Perry and Schamel 1990; Bosworth 1995).

The Gulf of Suez is comprised of three along-strike-linked sub-basins, separated by complex accommodation or transfer zones (Fig. 4; Moustafa 1976; Bosworth 1985; Jarrige et al. 1990; Patton et al. 1994; Moustafa 1997). Each of these sub-basins is a mega-half graben, with the large basin-bounding faults switching sides from south to north. The internal structure of each mega-half graben is dominated by nested, rotated fault blocks defined by sets of synthetic faults (Colletta et al. 1988; Perry and Schamel 1990; Patton et al. 1994; Bosworth and McClay 2001).

3.2 Present-Day Stress Fields

Borehole breakout studies in industry exploration wells indicate that the minimum horizontal stress (S_{hmin}) in the southern Gulf of Suez is presently aligned ~NNE-SSW, parallel to the relative slip trajectory of Sinai versus Arabia along the Gulf of Aqaba transform plate boundary (Fig. 4; Bosworth and Taviani 1996; Badawy 2001). A similar orientation is observed in the accommodation zone boundary between the Central and Darag (northern) sub-basins (Bosworth and Durocher 2017). By contrast, breakout and drilling-induced fracture data indicate NE-SW rift-normal extension in the Central sub-basin (Fig. 4).

A variety of models have been proposed regarding Miocene syn-rift stress fields in the Gulf of Suez, but most fault kinematic indicators suggest that NE-SW extension predominated (reviewed in Bosworth and McClay 2001). The subsurface present-day stress data indicate that the central sub-basin is continuing to extend in a manner essentially unchanged from the Miocene period of active continental rifting (Bosworth and Durocher 2017). The situation is very different in the Southern sub-basin, and in the boundary region between the Darag and Central sub-basins. In these areas the NNE-SSW S_{hmin} is compatible with GPS-derived NNW movement of the Sinai micro-plate as discussed above. Bosworth and Taviani (1996) suggested that the NNE-SSW S_{hmin} orientation did not appear in the southern Gulf of Suez until during the late Pleistocene, but before formation of the 125 ka MIS5e terraces discussed below.

Additional stress field data are needed to fully assess the sub-regional stress field variations in the Gulf of Suez. Based on the well data compiled in Fig. 4, it can be concluded that each of the sub-basins possesses a distinct shallow crustal present-day stress field and that the boundaries between these stress domains correspond to major fault geometries inherited from the main phase of Miocene continental rifting (Bosworth and Durocher 2017).

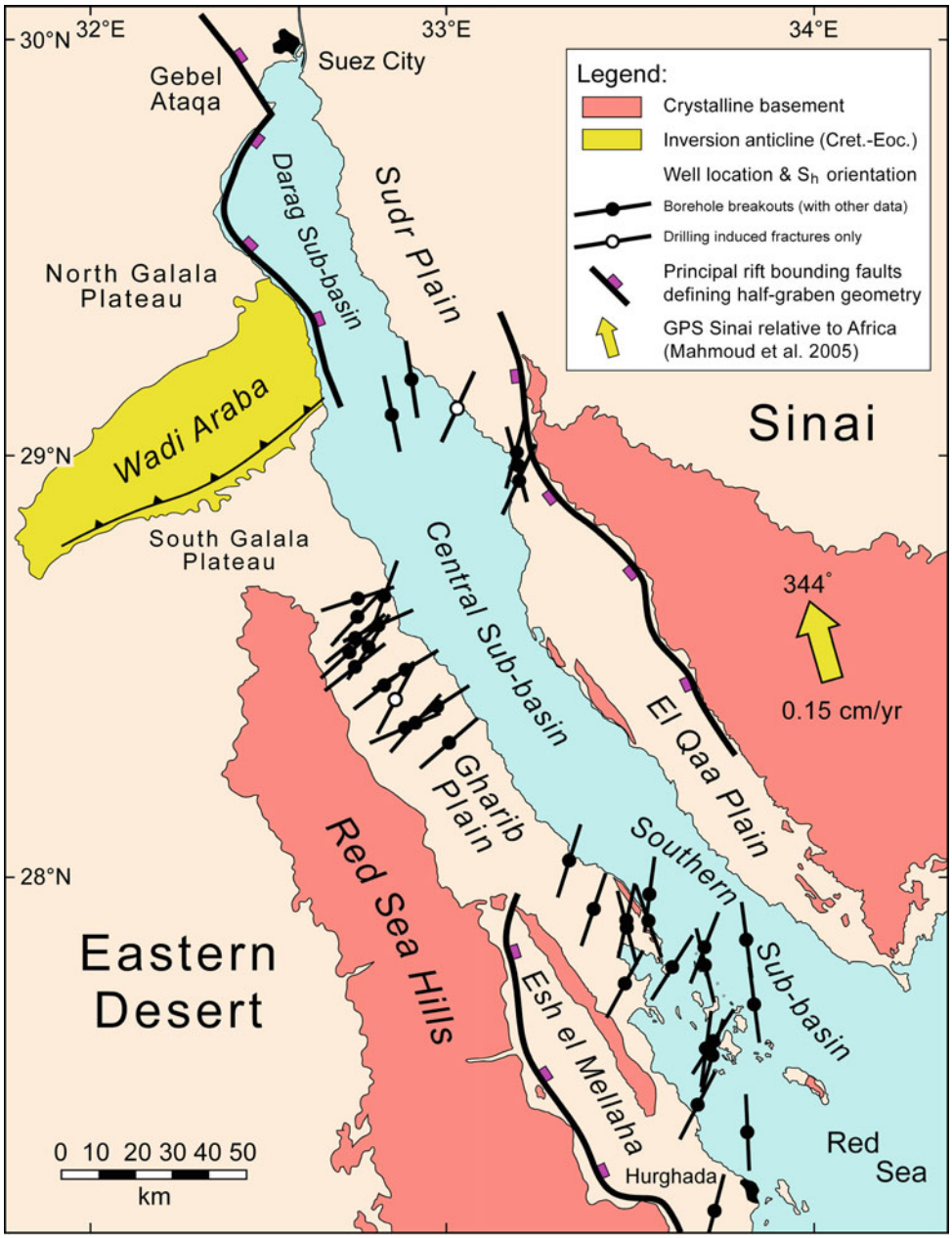

Fig. 4 Borehole breakout and drilling induced fracture data for the Gulf of Suez (Bosworth and Taviani 1996; Bosworth and Durocher 2017). Sticks show average S_{hmin} orientation for each well. The GPS-derived total vector of Sinai movement relative to Africa (Nubia) of ~0.15 cm/yr in the direction of 344° is adapted from Mahmoud et al. (2005). For simplicity only the rift-bounding faults are shown (boxes on downthrown side). The Wadi Araba inversion anticline formed in the Late Cretaceous to Late Eocene

3.3 Coral Terraces

Sea-level fluctuations during the Pleistocene resulted in the formation of several high-stand, interglacial coral terraces in the southern Gulf of Suez, the best preserved being the 125 ka MIS5e ('Eemian' or 'Ipswichian'; Fig. 5) (Andres and Radtke 1988; Reyss et al. 1993; Choukri et al. 1995). A detailed probabilistic and physical modeling approach has suggested that the MIS5e global sea level was 7.2 ± 1.3 m higher than at the present-day (Kopp et al. 2009). Following Kopp et al. we assume in our calculations that the MIS5e eustatic sea level was +7 m. Measurements of terrace elevations should ideally take into account a real-time tidal correction, and consideration of what the actual paleo-water depth for the measured feature was. Live corals are a truer indicator of the low-tide mark rather than average sea level, for example, and their position slightly underestimates the paleo-sea level elevation. But the Gulf of Suez, Gulf of

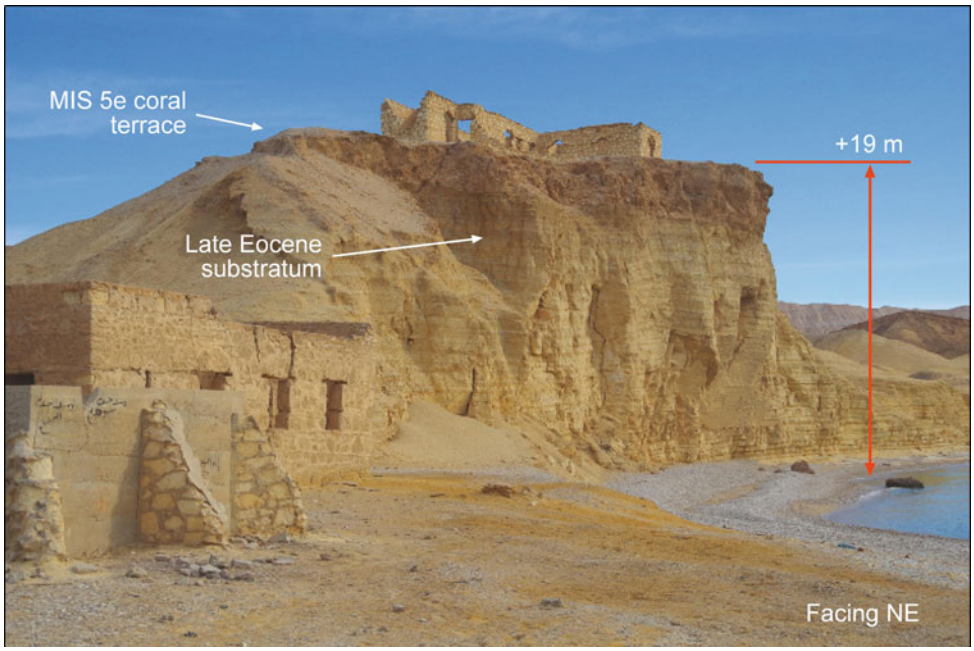

Fig. 5 MIS5e coral terrace at Gebel Tanka, north-central Gulf of Suez. The Pleistocene corals developed on an unconformity at the top of the Late Eocene Tanka Formation, which is comprised of thin-bedded shallow marine limestone. Gebel Tanka is in the uplifted and exposed footwall of a large Miocene-age extensional fault. The entire syn-rift and a small amount of the pre-rift stratigraphic section are absent at this locality. This is the highest recorded elevation for a MIS5e terrace in the Gulf of Suez. Location is shown on Fig. 6

Aqaba and Red Sea are generally micro-tidal environments today, with typical tidal ranges of less than one metre. Detailed tide charts are often not readily available for much of the coastline. Furthermore, minor erosion has affected many of the terraces. Other workers have discussed these considerations in more detail (Manaa et al. 2016; Inglis et al., this volume). Our analyses of the tectonic significance of the Pleistocene terraces are therefore minimum estimates of paleo-elevation and incur uncertainties of ~1 m (tidal range) beyond those of the actual measuring technique (LiDAR, tape measure, etc.).

A further complexity that might affect the differentiation of tectonic and eustatic signals in the coral terrace dataset is the role of regional isostacy driven by the episodic transfer of mass between the World ocean and continental ice sheets during the Pleistocene. Lambeck et al. (2011) referred to these effects as "glacio-hydro-isotatic contributions". The magnitude of this component of local sea level changes depends on the rheology of the underlying mantle and may be significant even far from the areas that were temporarily glaciated (Lambeck and Chappell 2001). Taking glacio-hydro-isostacy into consideration, Lambeck et al. (2011) estimated that for most of the greater Red Sea region the MIS5e sea level was only 1–2 m above the present-day level.

By surveying numerous MIS5e sites in the southern Gulf of Suez a view of post-125 ka relative subsidence or uplift can be established (Fig. 6; Bosworth and Taviani 1996). Ignoring the effects of isostacy, subtracting 7 m from these observations gives net tectonic change; including the Lambeck et al. glacio-hydro-isostatic contributions requires subtracting only about 2 m.

The MIS5e terraces record apparent footwall uplift of several major faults in the Gulf of Suez (Fig. 6). In the southern Gulf the maximum elevation of ~18.5 m is reached at Gebel el Zeit. Movement on the Gebel el Zeit fault is linked or transferred to another fault to the south that runs just east of Shadwan Island (Fig. 6). The Gebel el Zeit—Shadwan Island fault complex is seismically active (Jackson et al. 1988; Bosworth and Taviani 1996). Terrace elevations are not available for Shadwan Island itself but crystalline basement is exposed there and the crest of the fault block has risen at least relative to the surrounding basin.

MIS5e terrace elevations have not been determined for the Central Gulf of Suez north of Ras Shukeir (Fig. 6). On the east side of the Gulf, basement is exposed at Gebel Araba and patches of MIS5e coral complexes have been reported (Gvirtzman et al. 1992). These are heavily eroded and no terrace elevations were reported, but it is likely that this fault block is also undergoing some footwall uplift. Well-developed coral terraces are present in the northern part of the Central sub-basin at Gebel Tanka (Fig. 5) and less-developed terraces extend north of Hammam Faraun (Fig. 6). The Gebel Tanka terrace sits at +19 m, comparable to the north end of Gebel el Zeit. Unlike the Gebel el Zeit—Shadwan Island fault, the Hammam Faraun—Gebel Tanka

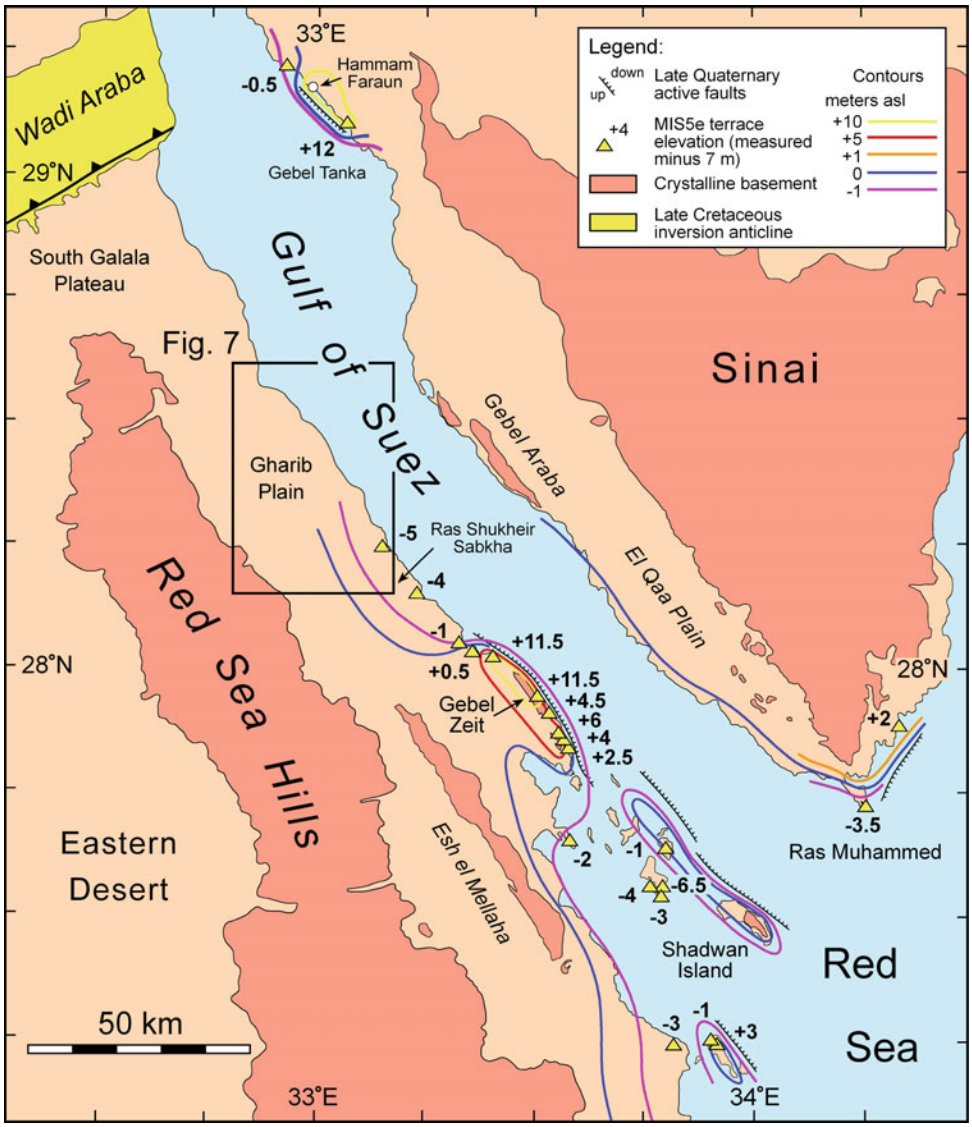

Fig. 6 Net tectonic movement of the MIS5e (Eemian, ~125 ka) coral terraces of the Gulf of Suez. The stated elevations are net tectonic movement after correcting for the +7 m MIS5e paleo-sea level. Glacio-hydro-isostacy considerations suggest that ~5 m should be added to each of the station values (Lambeck et al. 2011) Modified and extended from Bosworth and Taviani 1996. Locations of Fig. 5 (Gebel Tanka) and Fig. 7 (box) are shown

fault has not displayed historical seismicity, but this is certainly a long-term possibility. It is interesting to note that *both* active faults display strong oil and gas seeps at the coastline.

The Gebel el Zeit and Gebel Tanka terraces yield tectonic uplift rates of ~0.01 cm/yr without a glacio-hydro-isostatic correction, or 0.014 cm/yr with a correction.

3.4 Plio-Pleistocene Faulting

Despite the low extension rate (roughly an order of magnitude less than in the northern Red Sea), a broad belt of extensional faults developed along the central western margin of the Gulf of Suez in the Gharib alluvial plain (Fig. 7). Associated surface fault-line scarps are formed in partially lithified sands and gravels. The scarps are largely uneroded except where cut by the active wadi (dry river) systems. Trenching confirmed that the topographic scarps coincide with extensional faults with at least metres of offset. The deformed sands and gravels overlie Late Miocene evaporite beds and are themselves overlain by the MIS5e terraces. Their age is therefore post-Miocene to early-Pleistocene. The deformation appears to have been purely dip-slip although no fault plane kinematic data have been observed. The faults are very straight with an average strike of 145°. The Gharib fault

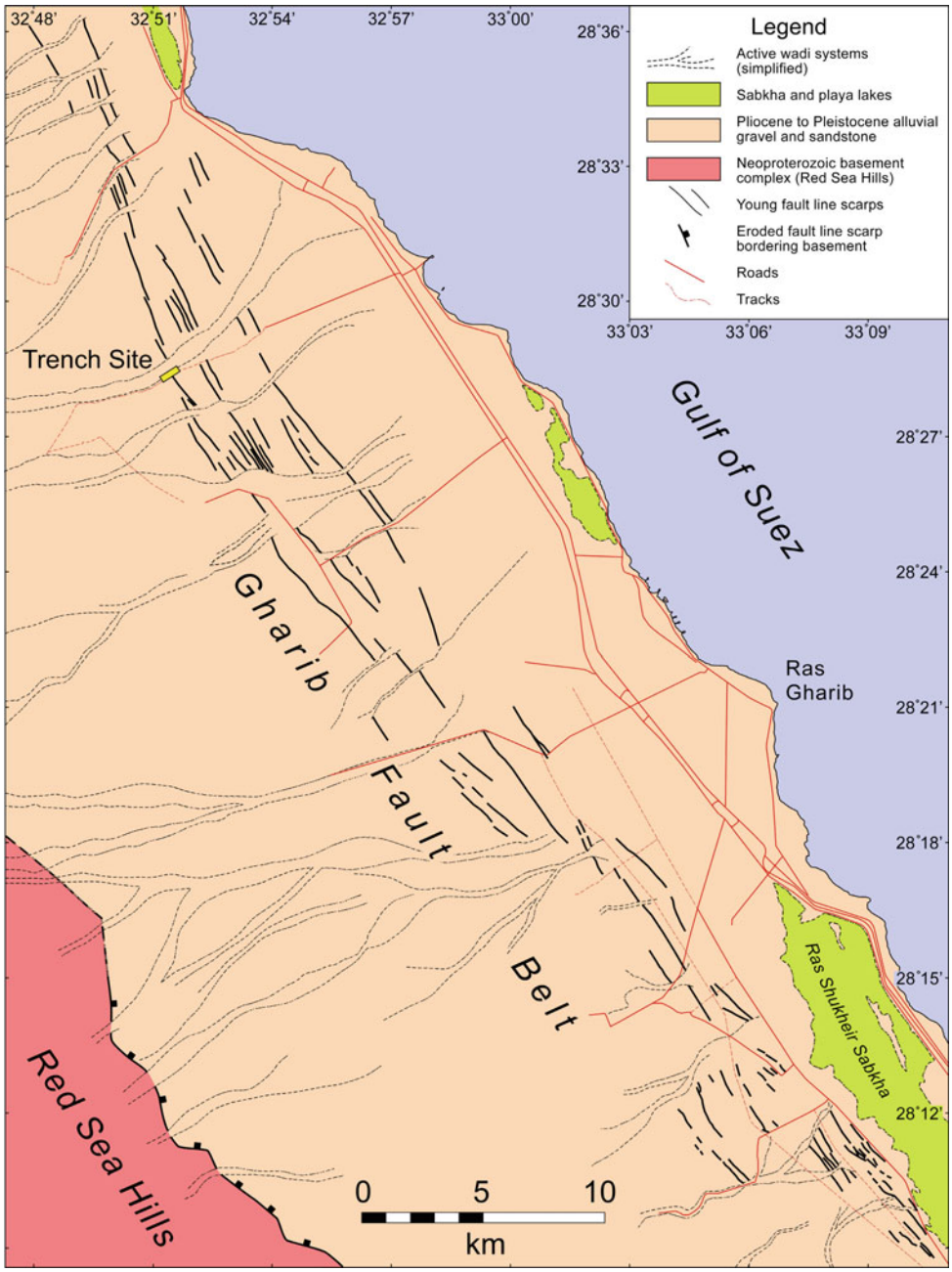

Fig. 7 Young fault-line scarps in Pliocene-Pleistocene alluvium on the west flank of the central Gulf of Suez (Gharib fluvial plain). Faults are straight and most are down-thrown toward the NE. They do not resemble structures that would be associated with underlying salt movement. Labelled yellow bar indicates position of trenching

belt probably developed in a stress field similar to that present today in the Central sub-basin and accommodated rift-normal extension. Because this fault array lies above Late Miocene evaporites it is possible that none of the faults is directly linked to basement structures. However, the straight fault pattern is not suggestive of basin-ward mass wasting or three-dimensional flow above rising salt domes or ridges.

4 Gulf of Aqaba

The Gulf of Aqaba is the southernmost segment of the left-lateral transform boundary that now links the northern Red Sea to the Zagros-Bitlas collision in eastern Turkey (Ben-Avraham et al. 1979; Bartov et al. 1980; Garfunkel

1981; Eyal et al. 1981; Ben-Avraham 1985). The offshore basin consists of three rhombohedral-shaped, left-stepping sub-basins, each with one or more bathymetric deeps (Fig. 8). As discussed above, several of the basin-parallel boundaries of these rhombs experience numerous small and occasional large magnitude earthquakes with strike-slip focal mechanisms, suggestive of traditional pull-apart basin geometries. However, reflection seismic data indicate that left-lateral slip on the west side of the northern (Elat) sub-basin is now being transferred to slip on the east side by a smooth, curvilinear fault, rather than at an orthogonal extensional fault (Ehrhardt et al. 2005). Similar complexities may exist in the central and southern sub-basins.

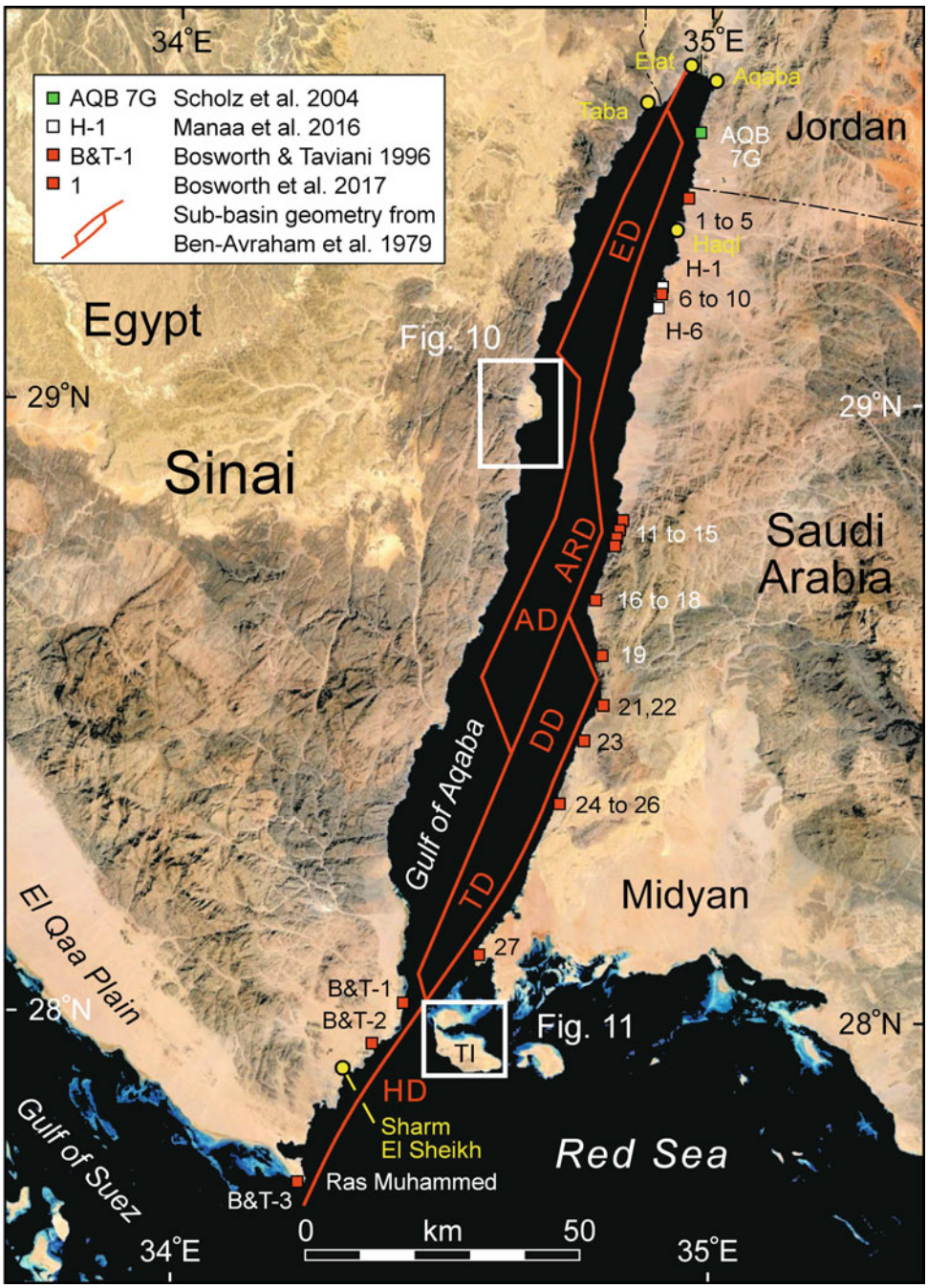

Fig. 8 Gulf of Aqaba MIS5e coral terrace and fault kinematics stations (Bosworth et al. 2017). Locations of Figs. 10 and 11 are shown by boxes. Sub-basin geometry and positions of bathymetric deeps are from Ben-Avraham et al. (1979). HD = Hume Deep; TD = Tiran Deep; DD = Dakar Deep; AD = Arnona Deep; ARD = Aragonese Deep; ED = Elat Deep; TI = Tiran Island. Basemap: Google Earth; Image Landsat

4.1 Present-Day Stress Fields

Industry exploratory wells have not yet been drilled in the Gulf of Aqaba so no borehole breakout data exist. The local present-day stress field can therefore only be interpreted from seismicity and outcrop fault kinematic data. Both large magnitude and small, locally recorded seismic events have been extensively analyzed in the Gulf of Aqaba and its onshore margins. Most $M_L \geq 5$ earthquakes have yielded left-lateral strike-slip focal mechanisms (Salamon et al. 1996; Roobol et al. 1999; Al-Tarazi 2000; Hofstetter 2003). Many of these large strike-slip events are concentrated in the Aragonese-Arnona deep (Fig. 8) and reflect the dominant movement of the Aqaba-Levant plate boundary. The simplest interpretation of these mechanisms suggests a NW-SE S_{Hmax}. However, smaller magnitude normal fault mechanisms are also recorded in local networks and in 1993 M_L = 5.8 and 5.6 predominantly normal-slip events occurred as part of a major earthquake swarm (Hofstetter 2003). These large events were located along the Arabian coastline of the Aragonese and Dakar deeps (Fig. 8) and indicated east-west extension. Similarly to the GPS datasets discussed above, seismicity supports the leaky transform model of Ben-Avraham et al. (1979).

East-west extension is not compatible with NW-SE oriented S_{Hmax}. Ben-Avraham and Zoback (1992) analyzed the relationships between the orientations of S_{hmin} and S_{Hmax} and the ratio of the frictional strength of a strike-slip fault versus the shear stress at failure of the adjacent crust. They found that for very weak faults, one or the other of the principal stresses rotates into parallelism with the fault itself. In a convergent setting, S_{hmin} swings into the fault orientation, whereas in a divergent setting it is S_{Hmax} that swings toward the fault orientation. Regional plate geometries and kinematics have produced a divergent setting at the Gulf of Aqaba, causing S_{Hmax} to be aligned roughly N-S along parts of the basin. This facilitates local extension perpendicular to the plate boundary.

4.2 Coral Terraces

Both the western (Sinai) and eastern (Arabia) margins of the Gulf of Aqaba display flights of Pleistocene coral terraces comparable to those in the Gulf of Suez. Pre-MIS5e Pleistocene coral terraces along the Jordanian and Saudi Arabian margin attain maximum elevations of ~100 m above sea level (Dullo 1990; Dullo and Montaggioni 1998). Pleistocene reef complexes are found up to 35 m above sea level in southeastern Sinai, although the upper surfaces of these highest reef terraces have been eroded (Gvirtzman et al. 1992).

Exposures of the MIS5e terrace are very extensive on the eastern margin of the Gulf of Aqaba, from near the city of Aqaba, Jordan, south to Midyan (Fig. 8). Elevations of the terraces are ~10 m in Jordan, rise to ~19–26 m in the central sub-basin margin, and then decline to ~9 m in Midyan (Fig. 9; Scholz et al. 2004; Manaa et al. 2016; Bosworth et al. 2017; Taviani et al., this volume).

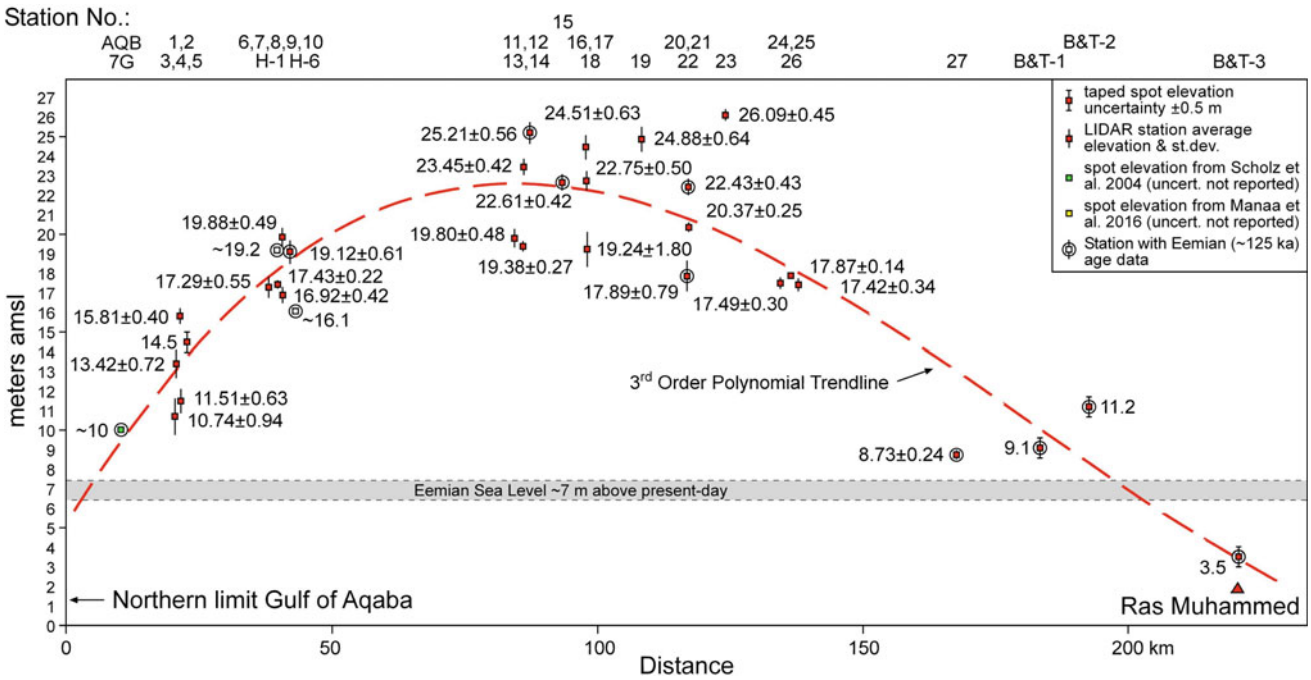

Fig. 9 Gulf of Aqaba MIS5e coral terrace elevations plotted along a north-south section. Station locations are shown in Fig. 8. Elevations are for the tops of the terraces relative to local sea level and without tidal corrections. After Bosworth et al. (2017)